

Families of discrete circular distributions with some novel applications ^{*}

Kanti V. Mardia[†] Karthik Sriram[‡]

Abstract

Motivated by some cutting edge circular data such as from Smart Home technologies and roulette spins from online and casino, we construct some new rich classes of discrete distributions on the circle. We give four new general methods of construction, namely (i) maximum entropy, (ii) centered wrapping, (iii) marginalized and (iv) conditionalized methods. We motivate these methods on the line and then work on the circular case and provide some properties to gain insight into these constructions. We mainly focus on the last two methods (iii) and (iv) in the context of circular location families, as they are amenable to development of a general methodology. We show that the marginalized and conditionalized discrete circular location families inherit some important properties from their parent continuous families. The resulting discrete families are also symmetric and have again two parameters akin to the mean direction and concentration parameter. In particular, for the von Mises and wrapped Cauchy as the parent distribution, we examine their properties including the maximum likelihood estimators, the hypothesis test for uniformity and give a test of serial independence. Using our discrete circular distributions, we demonstrate how to determine changepoint when the data arise in a sequence and how to fit mixtures of this distribution. Illustrative examples are given which triggered the work. For example, for roulette data, we test for uniformity (unbiasedness), test for serial correlation, detect changepoint in streaming roulette-spins data, and fit mixtures. We analyse a smart home data of human activities including fitting of our mixtures. In practice, the choice between marginalized approach and conditionalized methods is driven by the type of population. Further, choice between members of a given marginalized or conditionalized discrete family is usually data driven but we give a rule of thumb on different choices. We give various extensions of the families with skewness and kurtosis, to those supported on an irregular lattice, and discuss potential extension to general manifolds by showing a construction on the torus.

Keywords: changepoint; conditionalized distributions; entropy; Kullback-Leibler divergence; marginalized distributions; mixtures; multivariate; regular lattice; roulette data; skew;

^{*}This paper was presented at the LASR 2019

[†]University of Leeds and University of Oxford

[‡]Indian Institute of Management Ahmedabad, India.

smart home technology; stable distributions; torus; von Mises distribution; wrapped Cauchy distribution.

1 Introduction

Since the discussion paper of Mardia (1975a), the subject of directional data, as expected has grown tremendously with the focus on “statistics on manifolds” leading to new distributions on hyper-sphere, torus, Stiefel manifold, Grassmann manifold and so on. The progress in this area can be seen through several books since then: Fisher (1993), Fisher et al. (1987), Mardia and Jupp (2000), Jammalamadaka and Sengupta (2001), Ley and Verdebout (2017) and Ley and Verdebout (2018). Further, recently Pewsey and García-Portugués (2020) have given a comprehensive survey of the field. However, as far as we could trace, it seems no work on constructing families of discrete distributions has appeared even for the circular case. This paper lays the foundation for constructing families of discrete circular distributions, which can be further extended to higher manifolds.

For circular data, there are now good choices for continuous models but for the discrete data even such as modeling roulette wheel data (possibly biased) from gaming industries, there is a dearth of good models. The same comment applies to smart home monitoring for elderly. In this paper, we give four plausible methods to construct families of discrete distributions on the circle. The approaches to obtain the probability distribution under these methods can be briefly described as follows.

- (i) Maximum entropy method: determine the discrete probability distribution which has the maximum Shannon entropy among all those satisfying a set of moment constraints.
- (ii) Centered wrapping method: start with a discrete distribution on the line and wrap it on the circle.
- (iii) Marginalized method: start with a continuous circular distribution, which we refer to as the “parent” and obtain the discrete distribution by integrating the probability density function (pdf) on pre-determined intervals on the circle.
- (iv) Conditionalized method: start with a continuous circular distribution as the parent and obtain the distribution by restricting the pdf to a pre-determined lattice on the circle, and normalize.

The maximum entropy method arises as an adaptation of such construction for continuous distributions given in Mardia (1975a) and we show that it leads to general exponential families; the entropy definition can be modified to include non-exponential distributions. The wrapping of integer valued distributions, which was proposed in (Mardia, 1972, e.g. p. 54-55) usually do not have a natural centering parameter, but can be modified to include one. The next two methods start with a continuous distribution on the circle and then apply two different discretization approaches, viz. “marginalized” and “conditionalized”. We show that the latter three approaches are interrelated through a duality-theorem, wherein discretizing on the line and then wrapping on the circle leads to the same distribution as first wrapping and then discretizing.

For our discussion on inference and application to the real data examples, we select the marginalized and conditionalized approaches, as they are amenable to development of a general methodology required for inference, as well as more involved problems such as changepoint

analysis and fitting of mixtures. However, we note that the particular distributions we consider for our data applications also happen to arise as special cases from one of the other two methods. We describe the marginalized and conditionalized approaches in general for symmetric location families on the circle, and in particular apply to two main circular distributions, viz. von Mises (VM) and wrapped Cauchy (WC). Both of these continuous distributions have two parameters, namely “mean direction parameter” and “concentration parameter” (equivalently precision). These two cover two contrasting features with von Mises in exponential family and wrapped Cauchy not in exponential family but heavy tailed, and used mainly for M-type estimators.

The choice between methods, marginalized versus conditionalized, ideally depends on the nature of the data, i.e. grouped versus naturally discrete, but we will give evidence that the two methods turn out to be close except in the case of very small lattice supports. Similarly, the choice between different distributions arising from a particular method applied to different parent distributions (e.g. VM versus WC), depends on what best fits the practical application. However, it is possible that under some conditions the distributions albeit different may be practically indistinguishable leading to similar results. For conditionalized discrete distributions, we quantify such similarities by considering the Kullback-Liebler, L_1 and L_2 divergence metrics. We carry out different comparisons, between discrete versus continuous, between distributions from different methods as well as within a given method. Similar results are obtained for the marginalized discrete distributions; in particular, we note that for our specific data examples, the marginalized and conditionalized methods happen to yield similar conclusions.

We now give the two data examples which have motivated the paper though the subject is very broad. The data outcomes are supported on $r \in \{0, 1, \dots, m - 1\}$ corresponding to the circular lattice

$$\{2\pi r/m \quad : \quad r = 0, 1, \dots, m - 1\}.$$

Roulette wheel data: A typical European roulette is shown in Figure 1, which has $m = 37$ discrete outcomes, viz. $\{0, 1, 2, \dots, 36\}$. A problem of interest to a regulator as well as a casino is to ensure by regular monitoring that the roulette wheel remains unbiased, and detect a bias as quickly as possible based on streaming outcomes. For example, the UK Gambling Commission requires statistical testing to ensure fairness, and that the testing should be performed by an approved third party (see page 4 of the documentation on Testing strategy for compliance with remote gambling and software technical standards at <http://www.gamblingcommission.gov.uk/>.) We consider data sequences obtained from spins of three different European roulette wheels, one from an online roulette simulator and two from a casino industry.

Smart home eating activity data: One of the main sources of smart home data is the Environmental Protective Agency’s (EPA) “Consolidated Human Activity Database (CHAD)” . Various studies have appeared, and Chinellato et al. (2017) have given a brief description of the CHAD data base and reviewed some recent studies. In particular, they point out that normally the data is periodic (daily/ hourly measurements) and use a mixture of von Mises distributions. However, smart home sensors usually record half hourly or hourly measurements. In smart home industries such discrete data are often recorded, e.g. HOWZ: A smart home for the elderly (HOWZ). For illustrative purpose, we study the data taken extracted



Figure 1: European roulette wheel, where $m = 37$ used in our real examples.

from CHAD on eating habit activity of a household over a period of about one year recorded at half-hour intervals during the day, hence $m = 48$.

The roulette application is naturally discrete and conditionalized method would be a natural consideration to model such outcomes. In the smart-home application, the half-hour discretization of the clock is “artificial” in the sense of aggregation and hence it is preferable to use a model based on a parent continuous distribution so the marginalized method would be natural.

Section 2 gives the different methods of constructing discrete circular distributions, along with some results interrelating them. Section 3 gives some properties of the marginalized and conditionalized distributions, both in general as well as some specific to families arising from the cardioid, von Mises and wrapped Cauchy distributions. In Section 4, we study inference including maximum likelihood estimation and hypothesis test for uniformity, based on marginalized and conditionalized distributions, also making some comparisons with the continuous case. Practical applications also involve changepoint detection and fitting mixture of distributions and we put forward Bayesian solutions for these in Section 5. Section 6 deals with two practical examples. Our first example uses one real online as well as two casino roulette wheel data to determine presence of bias, and the other example is from smart home eating habit activity data from a well established data base (CHAD). In Section 7, we provide some comparative studies between continuous versus discrete, between type of methods: marginalized versus conditionalized, and distributions arising from a particular method. In Section 8, first we give a construction which extends the distributions to those supported on irregular lattice. Next, we extend the marginalized and conditionalized distributions to tractable and interpretable general families of distributions, which allows also for skewness and kurtosis. We also indicate how to construct discrete distribution on the torus, a starting point for potential future work on manifolds. We conclude the paper with a discussion in Section 9. The detailed proofs of all the results are given in the supplement.

2 Constructions of circular discrete distributions

In this section, we elaborate on the four different methods of construction of circular distributions mentioned in the introduction. We would like the distributions to be supported on a regular circular lattice. By way of notation, we will denote the set of real numbers by \mathbb{R} , non-negative real numbers by \mathbb{R}^+ , the set of integers by \mathbb{Z} , non-negative integers by \mathbb{Z}^+ and

the cyclic group of integers modulo (a given positive integer) m by

$$\mathbb{Z}_m = \{0, 1, \dots, m-1\}. \quad (1)$$

The circular lattice domain of interest is \mathbb{Z}_m , or equivalently the set of vertices of a regular polygon on the circle, which can be written as

$$\mathcal{D}_m = \{2\pi r/m, r \in \mathbb{Z}_m\}. \quad (2)$$

We generally use $f(\cdot)$ or $g(\cdot)$ to denote a probability density function (pdf) of a continuous distribution on the line or circle and $p(\cdot)$ to denote a discrete probability function on integers.

2.1 Maximum entropy discrete circular distributions

For a probability function $\{p_r, r \in \mathbb{Z}_m\}$, with p_r denoting the probability of the point $2\pi r/m \in \mathcal{D}_m$, Shannon's entropy is defined as

$$-\sum_{r=0}^{m-1} p_r \log p_r. \quad (3)$$

Let t_1, t_2, \dots, t_q be real valued functions defined on \mathbb{Z}_m and suppose we are interested in discrete distributions that satisfy the moment conditions

$$E(t_1(r)) = a_1, E(t_2(r)) = a_2, \dots, E(t_q(r)) = a_q. \quad (4)$$

Then a useful method to construct discrete distributions is to maximize the entropy among all distributions on the given support that satisfy the given moment conditions. As noted in Kemp (1997), the philosophy behind this construction is that "one should use all the given information and nothing else". The following theorem gives this construction, which is the result of Mardia (1975a) adapted here to the circular discrete case.

Theorem 1 (Maximum Entropy Distributions). *The probability function supported on \mathcal{D} that maximizes the entropy (3) subject to the constraints (4) is of the form*

$$P(2\pi r/m) = \frac{e^{\sum_{i=1}^q b_i t_i(r)}}{\sum_{k=0}^{m-1} e^{\sum_{i=1}^q b_i t_i(k)}}, \quad r \in \mathbb{Z}_m, \quad (5)$$

provided there exist constants b_1, b_2, \dots, b_q satisfying

$$\frac{\sum_{r=0}^{m-1} t_j(r) e^{\sum_{i=1}^q b_i t_i(r)}}{\sum_{k=0}^{m-1} e^{\sum_{i=1}^q b_i t_i(k)}} = a_j, \quad j = 1, 2, \dots, q. \quad (6)$$

Further, if they exist then the distribution is unique.

We now give a few examples of maximum entropy discrete distributions.

Example 1. von Mises distribution: Suppose $q = 2$ and $t_1(r) = \cos(2\pi r/m)$ and $t_2(r) = \sin(2\pi r/m)$, the maximum entropy distribution is of the form

$$p(r) = \frac{e^{\kappa \cos(2\pi r/m - \mu)}}{\sum_{k=0}^{m-1} e^{\kappa \cos(2\pi k/m - \mu)}}, \quad r \in \mathbb{Z}_m, \quad (7)$$

where $\kappa = \sqrt{b_1^2 + b_2^2}$ and $\tan \mu = b_2/b_1$.

Example 2. Beran distributions: A more general family than the previous example, a discrete version of Beran family (Beran 1979) is obtained by considering constraints on expected values of $t_k(r) = (\cos(k2\pi r/m), \sin(k2\pi r/m))$, which leads to the probability function

$$p(r) \propto e^{\sum_{k=1}^q (a_k \cos(k2\pi r/m) + b_k \sin(k2\pi r/m))}. \quad (8)$$

Example 3. Geometric distribution: Suppose $q = 1$ and $t_1(r) = r$ the maximum entropy distribution is of the form

$$p(r) = \frac{(1-p)p^r}{1-p^m}, \quad r \in \mathbb{Z}_m, \quad \text{where } p = e^{b_1}. \quad (9)$$

The above three examples also arise out of the “conditionalized” construction of discrete circular distributions that we later define in this paper. Further, (9) is the “centered wrapped geometric distribution” discussed below. However, the maximum entropy construction can lead to more general subclasses of the exponential family of distributions, which we do not pursue in this paper. Further, distributions can be constructed by maximizing differential entropy on extending the work on the continuous circular case for example the properties of wrapped Cauchy distributions given in Kato and Pewsey (2015).

2.2 Centered wrapped discrete circular distributions

A natural construction to obtain a circular discrete distribution is to start with a discrete distribution on the line and wrap it on the circle (see Mardia 1972, p.50). Let $p(\cdot)$ be a probability distribution on integers $z \in \mathbb{Z}$. We get the wrapped distribution

$$z_w = z(\text{mod } m)2\pi/m \in \mathcal{D}_m,$$

and the probability function of z_w is given by

$$P(z_w = 2\pi r/m) = p_w(r) = \sum_{k=-\infty}^{\infty} p(r + km), \quad r \in \mathbb{Z}_m. \quad (10)$$

It follows that the characteristic function of z_w is given by

$$\psi_p = \phi(2\pi p/m). \quad (11)$$

where $\phi(\cdot)$ is the characteristic function of z .

In general, these distributions do not have a mean direction or centering parameter and therefore we introduce a centering parameter t as follows

$$P(z_w = 2\pi r/m) = p_w(r) = \begin{cases} p_w(r - t + m), & r < t \\ p_w(r - t), & r \geq t, \end{cases} \quad r, t \in \mathbb{Z}_m. \quad (12)$$

Choosing the domain of t as \mathbb{Z}_m ensures probabilities are well defined without changing the domain of the distribution. Some examples are given below.

Example 4. Centered wrapped Poisson distribution: If x has the Poisson distribution with mean λ , then from equation (10), x_w has the wrapped Poisson distribution with the probability function

$$p_{w0}(r) = e^{-\lambda} \sum_{k=0}^{\infty} \frac{\lambda^{r+km}}{(r+km)!}, \quad r \in \mathbb{Z}_m. \quad (13)$$

The probability function with centering parameter t is then given by

$$p_w(r) = \begin{cases} e^{-\lambda} \sum_{k=0}^{\infty} \frac{\lambda^{r-t+m+km}}{(r-t+m+km)!}, & r < t \\ e^{-\lambda} \sum_{k=0}^{\infty} \frac{\lambda^{r-t+km}}{(r-t+km)!}, & r \geq t \end{cases} \quad r, t \in \mathbb{Z}_m. \quad (14)$$

This is a special case of distributions considered by Mastrantonio et al. (2019).

Example 5. Centered wrapped skew Laplace distribution: The probability function of discrete skew Laplace (see for example Jayakumar and Jacob 2012) is given by

$$p(k) = \frac{(1-p)(1-q)}{1-pq} \times \begin{cases} p^k, & k = 0, 1, 2, \dots \\ q^{-k}, & k = 0, -1, -2, \dots \end{cases}, \quad p, q \in (0, 1). \quad (15)$$

From equation (10)

$$p_{w0}(r) = \frac{(1-p)(1-q)}{1-pq} \left(\frac{p^r}{1-p^m} + \frac{q^{m-r}}{1-q^m} \right), \quad r \in \mathbb{Z}_m, \quad (16)$$

and the probability function with centering parameter is given by

$$p_w(r) = \begin{cases} \frac{(1-p)(1-q)}{1-pq} \left(\frac{p^{r-t+m}}{1-p^m} + \frac{q^{t-r}}{1-q^m} \right), & r < t \\ \frac{(1-p)(1-q)}{1-pq} \left(\frac{p^{r-t}}{1-p^m} + \frac{q^{m-r+t}}{1-q^m} \right), & r \geq t \end{cases} \quad r, t \in \mathbb{Z}_m. \quad (17)$$

Example 6. Centered wrapped geometric distribution: The probability function of the geometric distribution is given by

$$p(k) = p^k(1-p), \quad k \in \mathbb{Z}^+, \quad p \in (0, 1). \quad (18)$$

From equation (10) we have

$$p_{w0}(r) = \frac{(1-p)p^r}{1-p^m}, \quad r \in \mathbb{Z}_m. \quad (19)$$

Mardia (1972, p. 50) proposed the wrapped geometric distribution as a model for (possibly biased) roulette outcomes. For a roulette wheel having $m = 2n + 1$ points with bias at $\theta = 0$, an alternative form for the wrapped geometric model was given as:

$$P(\theta = 2\pi|r|/m) \propto p^{(r+1)}, \quad |r| = 0, 1, \dots, m, \quad (20)$$

Equation (20) can be obtained by a simple change the domain. The probability function of the centered wrapped geometric distribution is given by

$$p_w(r) = \begin{cases} \frac{(1-p)p^{r-t+m}}{1-p^m}, & r < t \\ \frac{(1-p)p^{r-t}}{1-p^m}, & r \geq t \end{cases} \quad r, t \in \mathbb{Z}_m. \quad (21)$$

2.3 Marginalized and conditionalized discrete distributions

We first motivate the marginalized and conditionalized methods of constructions on the line and then we apply to the circle.

2.3.1 Preliminaries: constructions on the line

Let $f(x)$ be a pdf on \mathbb{R} , which satisfies some regularity conditions. We call f as the parent distribution, and describe two methods, namely “marginalized” and “conditionalized” as ways to construct discrete distributions from it. Both methods lead to discrete distributions supported on $r \in \mathbb{Z}$.

Definition 1. *The probability function of the marginalized discrete (MD) distribution on the line is obtained by integrating the pdf in each interval, and is given by*

$$p(r) = \int_r^{r+1} f(x)dx, \quad r \in \mathbb{Z}. \quad (22)$$

Definition 2. *The probability function of the conditionalized discrete (CD) distribution on the line is obtained by conditioning $x = r$ (i.e. plugging in $x = r$) in the pdf and normalizing, and is given by*

$$p(r) = \frac{f(r)}{\sum_{r=-\infty}^{\infty} f(r)}, \quad r \in \mathbb{Z}. \quad (23)$$

Of course, with appropriate modification, the domain of the discrete distribution can be generalized to $c + \delta\mathbb{Z}$, for some $\delta, c \in \mathbb{R}$. Also, the same procedure can be applied to non-negative domains. To understand these two constructions, let us consider two examples: one starting with the exponential distribution and the other with the Cauchy distribution.

Example 7. The pdf of the exponential distribution is given by

$$f(x) = \lambda e^{-\lambda x}, \quad x \geq 0, \quad \lambda > 0.$$

The marginalized discrete exponential distribution is given by

$$p(r) = \int_r^{r+1} \lambda e^{-\lambda x} dx = e^{-\lambda r}(1 - e^{-\lambda}) = p^r(1 - p), \quad p = e^{-\lambda}, \quad r \in \mathbb{Z}^+. \quad (24)$$

The conditionalized discrete exponential distribution is given by

$$p(r) \propto e^{-\lambda r}, \quad \text{or } p(r) = (1 - p)p^r, \quad p = e^{-\lambda} \quad r \in \mathbb{Z}^+. \quad (25)$$

Interestingly, if we start with the exponential distribution, both marginalized and conditionalized lead to the same discrete distribution, namely the geometric distribution. This leads to an interesting characterization theorem that the two approaches lead to the same distribution if and only if the parent is the exponential distribution. We also have an analogous results for the discrete circular case (see supplement).

Example 8. The pdf of Cauchy distribution is given by

$$f(x) = \frac{a}{\pi} \frac{1}{a^2 + x^2}, \quad x \in (-\infty, \infty), \quad a > 0.$$

The marginalized discrete Cauchy distribution is then given by

$$p(r) = \frac{1}{\pi} \left(\tan^{-1} \left(\frac{r+1}{a} \right) - \tan^{-1} \left(\frac{r}{a} \right) \right) = \frac{1}{\pi} \tan^{-1} \frac{a}{a^2 + r(r+1)}, \quad r \in \mathbb{Z}. \quad (26)$$

The conditionalized discrete Cauchy distribution (using Jolley (1961, p.22, equation (124)) is given by

$$p(r) = \frac{a \tanh(a\pi)}{\pi} \frac{1}{a^2 + r^2}, \quad r \in \mathbb{Z}. \quad (27)$$

So, for Cauchy distribution, marginalized and conditionalized discrete distributions are not the same.

There has been some scattered literature on the conditionalized discretization on the line, for example based on method (23), Kemp (1997) and Szabłowski (2001) discuss the conditionalized discrete normal, Inusaha and Kozubowski (2006) discuss the conditionalized discrete Laplace and Papadatos (2018) derives characteristic function of the conditionalized discrete Cauchy. The conditionalized approach can also be described as a “plug-in” approach, whereas the marginalized approach is in fact equivalent to the well known probit construction, usually used for univariate and multivariate normal distributions, see for example Joe (2014, p.20). However, this is the first time there is a unified treatment of these approaches as a strategy to construct rich classes of discrete distributions. We have dealt with only univariate distributions but the same constructions go through for multivariate distributions. Our focus is to give insight into these methods of construction and their ramifications, which are clear from dealing with the univariate case. Besides, our emphasis here is on the circular distributions.

2.3.2 Marginalized and conditionalized constructions on the circle

Following the above discussion, we now define the marginalized and conditionalized discrete families for the circular case. Let θ be a random variable with pdf $f(\theta)$, $\theta \in [0, 2\pi)$.

Definition 3. *The probability function of the marginalized discrete (MD) distribution on the circle is given by*

$$p(r) = \int_{\frac{2\pi r}{m}}^{\frac{2\pi(r+1)}{m}} f(\theta) d\theta = F \left(\frac{2\pi(r+1)}{m} \right) - F \left(\frac{2\pi r}{m} \right), \quad r \in \mathbb{Z}_m, \quad (28)$$

where $F(\cdot)$ is the cumulative distribution function of $f(\theta)$.

We note that this is also the probability function of the discrete random variable $\lfloor \frac{m\theta}{2\pi} \rfloor$, where $\lfloor \cdot \rfloor$ denotes the largest integer less than or equal to the given number.

Definition 4. *The probability function of the conditionalized discrete (CD) distribution on the circle is given by*

$$p(r) = \frac{f(2\pi r/m)}{\sum_{k=0}^{m-1} f(2\pi k/m)}, \quad r \in \mathbb{Z}_m. \quad (29)$$

For simplicity, we will denote both probability functions by the same notation, but the choice will be obvious from the context. One question of interest is whether the marginalized and conditionalized methods applied to a pdf f can lead to the same discrete distribution. Theorem 2 shows that if both the methods applied to pdf f result in the same discrete probability function on the line, then the methods applied to the f wrapped on the circle will also result in the same discrete probability function.

Theorem 2 (Marginalized and conditionalized distribution invariance).

Suppose f is a pdf on $[0, \infty)$ satisfying the condition

$$\frac{f(r\delta)}{\sum_{k=0}^{\infty} f(k\delta)} = \int_{r\delta}^{(r+1)\delta} f(x)dx, \quad \forall \delta > 0. \quad (30)$$

Let $f_w(\theta)$ be the pdf when f is wrapped on the circle. Then we have

$$\frac{f_w(2\pi r/m)}{\sum_{k=0}^{m-1} f_w(2\pi k/m)} = \int_{2\pi r/m}^{2\pi(r+1)/m} f_w(\theta)d\theta. \quad (31)$$

As seen in the previous section, for the exponential distribution, both marginalized and conditionalized methods lead to the same discrete distribution. It follows from Theorem 2 that the property also holds for the wrapped exponential on the circle. However, in general, the two approaches will lead to different distributions. There is also an interesting connection between the constructions on the circle and the line, which is given by the following theorem.

Theorem 3 (Duality).

Let $X \sim f(\cdot)$ a pdf on \mathbb{R} . Consider the following two methods of constructing discrete circular distributions supported on \mathbb{Z}_m .

- (a) Discretize the random variable $\tilde{X} = mX/(2\pi)$ and denote it by \tilde{X}_d , and further denote its wrapped version ($\tilde{X}_d \bmod m$) by \tilde{X}_{dw} .
- (b) Wrap the random variable X as $X_w = (X \bmod 2\pi)$, and discretize the random variable $\tilde{X}_w = mX_w/2\pi$, denote it by \tilde{X}_{wd} .

For both the discretization methods, viz marginalized and conditionalized, the above two approaches lead to the same discrete distribution, i.e. \tilde{X}_{dw} and \tilde{X}_{wd} have the same distributions.

We now apply the marginalized and conditionalized methods starting with the von Mises and the wrapped Cauchy as the parent distributions. The basic circular distribution (analogue of the normal distribution on line) is the von Mises (VM) distribution (see, for example, Mardia and Jupp 2000, p.36), which has the pdf

$$f_v(\theta|\kappa, \mu) = \frac{1}{2\pi I_0(\kappa)} e^{\kappa \cos(\theta-\mu)}, \theta \in [0, 2\pi), \mu \in [0, 2\pi), \kappa \geq 0, \quad (32)$$

where μ is the mean direction, κ is the concentration parameter and $I_0(\kappa)$ is the modified Bessel function of order 0. Using equation (28), we can now define the marginalized discrete von Mises distribution (MDVM).

Definition 5. The probability function for the marginalized discrete von Mises (MDVM) distribution with mean parameter μ and concentration parameter κ is given by

$$p(r|m, \kappa, \mu) = \frac{1}{2\pi I_0(\kappa)} \int_{2\pi r/m}^{2\pi(r+1)/m} e^{\kappa \cos(\theta-\mu)} d\theta, r \in \mathbb{Z}_m, \quad \mu \in [0, 2\pi), \quad (33)$$

We note that this does not have a closed form. Starting with the pdf (32), we can define the conditionalized discrete von Mises (CDVM) as below.

Definition 6. *The probability function for the conditionalized discrete von Mises (CDVM) distribution with mean parameter μ and concentration parameter κ is given by*

$$p(r|m, \kappa, \mu) = \frac{1}{L_0(\kappa, \mu)} e^{\kappa \cos(2\pi r/m - \mu)}, r \in \mathbb{Z}_m, \mu \in [0, 2\pi), \quad (34)$$

where the normalizing constant is the reciprocal of the function

$$L_0(\kappa, \mu) = \sum_{r=0}^{m-1} e^{\kappa \cos(2\pi r/m - \mu)}. \quad (35)$$

Another distribution, which is becoming increasingly popular (see, for examples, Kato and Jones 2015, Kato and Pewsey 2015, and Kent and Tyler 1988) is the wrapped Cauchy (WC) distribution with the pdf given by (see, for example, Mardia and Jupp 2000, page 51)

$$f_c(\theta|\rho, \mu) = \frac{1}{2\pi} \frac{1 - \rho^2}{1 + \rho^2 - 2\rho \cos(\theta - \mu)}, \theta \in [0, 2\pi), \mu \in [0, 2\pi), \rho \in [0, 1), \quad (36)$$

where μ is the mean direction parameter and ρ is the concentration parameter. Here the cumulative distribution function has a closed form and based on the marginalization method in equation (28), we can define the probability function of the marginalized discrete wrapped Cauchy (MDWC) below.

Definition 7. *The probability function of marginalized discrete wrapped Cauchy (MDWC) with mean parameter μ and concentration parameter ρ is given by*

$$p(r|m, \rho, \mu) = \frac{1}{2\pi} \cos^{-1} \left\{ \frac{(1 + \rho^2) \cos(\frac{2\pi(r+1)}{m} - \mu) - 2\rho}{1 + \rho^2 - 2\rho \cos(\frac{2\pi(r+1)}{m} - \mu)} \right\} - \frac{1}{2\pi} \cos^{-1} \left\{ \frac{(1 + \rho^2) \cos(\frac{2\pi r}{m} - \mu) - 2\rho}{1 + \rho^2 - 2\rho \cos(\frac{2\pi r}{m} - \mu)} \right\} \quad r \in \mathbb{Z}_m. \quad (37)$$

Alternatively, this can be written as follows, the form which we will be using for computational purposes.

$$p(r|m, \rho, \mu) = \frac{1}{\pi} \arctan \left(\frac{\frac{1+\rho}{1-\rho} \{ \tan(\pi(r+1)/m - \mu/2) - \tan(\pi r/m - \mu/2) \}}{1 + \left(\frac{1+\rho}{1-\rho} \right)^2 \tan(\pi(r+1)/m - \mu/2) \tan(\pi r/m - \mu/2)} \right), \quad r \in \mathbb{Z}_m, \mu \in [0, 2\pi), \rho \in [0, 1). \quad (38)$$

Again, using equations (29) and (36), we have the following definition.

Definition 8. *The probability function of the conditionalized discrete wrapped Cauchy (CDWC) distribution with mean parameter μ and concentration parameter ρ is given by*

$$p(r|m, \rho, \mu) = \frac{(1 - 2\rho^m \cos(m\mu) + \rho^{2m})(1 - \rho^2)}{m(1 - \rho^{2m})} \frac{1}{1 - 2\rho \cos(\frac{2\pi r}{m} - \mu) + \rho^2}, \quad r \in \mathbb{Z}_m, \mu \in [0, 2\pi). \quad (39)$$

The normalizing constant of the probability function in (39) is derived in the supplement. For simplicity of notation, while writing the marginalized or conditionalized probability functions, we will omit the subscripts v or c corresponding to von Mises or Cauchy, but they will be clear from the context and by the explicit mention of κ versus ρ as the concentration parameters.

Without major loss of information, for mathematical and computational convenience, we take the mean direction parameter μ for discrete case as

$$\mu = 2\pi t/m, \quad t \in \mathbb{Z}_m, \quad (40)$$

and call t the ‘‘centering’’ parameter. However, all the data analysis in this paper can be suitably modified to allow for an unrestricted μ parameter. Accordingly, the probability function of MDWC (38) can be written as

$$p(r|m, \rho, \mu) = \frac{1}{\pi} \tan^{-1} \left(\frac{\frac{1+\rho}{1-\rho} \{\tan(\pi(r+1-t)/m) - \tan(\pi(r-t)/m)\}}{1 + \left(\frac{1+\rho}{1-\rho}\right)^2 \tan(\pi(r+1-t)/m) \tan(\pi(r-t)/m)} \right),$$

$$r, t \in \mathbb{Z}_m, \quad \rho \in [0, 1). \quad (41)$$

From equation (34) the corresponding conditionalized probability function for CDVM is given by

$$p(r|m, \kappa, t) = \frac{1}{L_0(\kappa)} e^{\kappa \cos(2\pi(r-t)/m)}, \quad r, t \in \mathbb{Z}_m, \quad \kappa \geq 0, \quad (42)$$

where normalizing constant is now free of the parameter t and is the reciprocal of

$$L_0(\kappa) = \sum_{r=0}^{m-1} e^{\kappa \cos(2\pi r/m)}. \quad (43)$$

Similarly, from equation (39) the corresponding probability function for CDWC is given by

$$p(r|m, \rho, t) = \frac{(1-\rho^2)(1-\rho^m)}{m(1+\rho^m)} \frac{1}{1 + \rho^2 - 2\rho \cos(2\pi(r-t)/m)},$$

$$r, t \in \mathbb{Z}_m, \quad \rho \in [0, 1). \quad (44)$$

We will write $r \sim MDVM(m, \kappa, t)$ and $r \sim MDWC(m, \rho, t)$ for the marginalized discrete von Mises and marginalized discrete wrapped Cauchy distributions respectively, if $t \neq 0$. If $t = 0$, we just omit t and write $r \sim MDVM(m, \kappa)$ and $r \sim MDWC(m, \rho)$. Similarly, we will write $r \sim CDVM(m, \kappa, t)$ and $r \sim CDWC(m, \rho, t)$ for the conditionalized discrete von Mises and conditionalized discrete wrapped Cauchy distributions respectively, if $t \neq 0$. If $t = 0$, we just omit t and write $r \sim CDVM(m, \kappa)$ and $r \sim CDWC(m, \rho)$. We will always denote the discrete probability functions by $p(r|m, \kappa, t)$ for von Mises or $p(r|m, \rho, t)$ for wrapped Cauchy, and if $t = 0$, we just write $p(r|m, \kappa)$ or $p(r|m, \rho)$. The distinction between von Mises and wrapped Cauchy can be made by the use of κ and ρ to denote the concentration parameters. Again for simplicity, we avoid separate notations for marginalized versus conditionalized probability functions but their use will be clear from the context.

2.4 Discrete circular distributions using copulas

Here, we briefly outline a strategy to construct multivariate discrete distributions using copulas. Suppose $f_1(\theta)$ and $f_2(\theta)$ are univariate pdfs on the circle, i.e. $\theta \in [0, 2\pi)$ and $f_1(\theta+2\pi) = f_1(\theta)$, $f_2(\theta+2\pi) = f_2(\theta)$. We consider the circular copulas of Johnson and Wehrly (1978), which has been further studied by Jones et al. (2015). Suppose F_1 and F_2 be the corresponding cdfs. Then the following bivariate density will have f_1 and f_2 as its marginals.

$$f(\theta_1, \theta_2) = 2\pi f_1(\theta_1) f_2(\theta_2) g(2\pi(F_2(\theta_2) - F_1(\theta_1))), \quad (45)$$

where $g(\cdot)$ is a univariate circular pdf on $[0, 2\pi)$.

The marginalized bivariate discrete probability function with (45) as parent can then be obtained as

$$\begin{aligned} p(r_1, r_2) &= \int_{2\pi r_1/m}^{2\pi(r_1+1)/m} \int_{2\pi r_2/m}^{2\pi(r_2+1)/m} f_1(\theta_1) f_2(\theta_2) g(2\pi(F_2(\theta_2) - F_1(\theta_1))) d\theta_2 d\theta_1 \end{aligned} \quad (46)$$

It is easy to verify that the marginal distributions of the marginalized bivariate discrete probability function are again the marginalized univariate probability functions.

The conditionalized bi-variate discrete probability function with (45) as parent is

$$p(r_1, r_2) = \frac{f_1(2\pi r_1/m) f_2(2\pi r_2/m) g(2\pi(F_2(2\pi r_2/m) - F_1(2\pi r_1/m)))}{\sum_{r_1=0}^{m-1} \sum_{r_2=0}^{m-1} f_1(2\pi r_1/m) f_2(2\pi r_2/m) g(2\pi(F_2(2\pi r_2/m) - F_1(2\pi r_1/m)))} \quad (47)$$

We explore these ideas further with a specific construction on the torus in Section 8.3.

3 Properties

We consider a general circular location family (see, for example, Mardia 1975b) with probability density function given by

$$f(\theta|\tau, \mu) = g_\tau(\theta - \mu), \quad \theta, \mu \in [0, 2\pi), \quad (48)$$

which we assume to be unimodal with mode at μ . For simplicity, we assume $g_\tau(\theta) = g_\tau(2\pi - \theta)$ for all $\theta \in [0, 2\pi)$ and also that $g_\tau(2\pi) = g_\tau(0)$, and $g_\tau > 0$. Note that the normalizing constant will depend only on τ and not on μ . Here, $\tau \geq 0$ is another parameter in addition to μ , such that $\tau = 0$ corresponds to the case of uniform distribution and the dispersion around the mode decreases as τ increases. For example, $\tau = \kappa$ for the von Mises distribution (32), and $\tau = \rho$ for wrapped Cauchy distribution (36). We will need some condition on first and second derivatives of $g_\tau(\cdot)$ to consider inference problems such as the maximum likelihood estimation etc. Here, we discuss some general properties of the marginalized and conditionalized discrete circular distributions arising from such location families.

3.1 Properties of marginalized discrete distributions

The probability function for the marginalized discrete distribution based on the circular location family (48) is given by

$$p(r|m, \tau, t) = \int_{2\pi r/m}^{2\pi(r+1)/m} g_\tau(\theta - 2\pi t/m) d\theta, \quad r, t \in \mathbb{Z}_m. \quad (49)$$

We will call this distribution the “marginalized discrete circular location family” and summarize its properties in the following theorem.

Theorem 4. *The marginalized discrete circular location family has the following properties inherited from the parent family (48), but with some variations.*

(a) *It has normalizing constant free of centering parameter t .*

(b) *It is not unimodal, but has two modes, at $r = t - 1$ and $r = t$.*

(c) *It is symmetrical about $(t - 1/2)$, and satisfies*

$$p(m - r - t|m, \tau, t) = p(r - 1 - t|m, \tau, t).$$

(d) *Its characteristic function (for integer $p \pmod{m}$) is*

$$E \left[e^{ip \frac{2\pi r}{m}} \right] = e^{ip \frac{2\pi t}{m}} \psi_{p,m}(\tau), \quad (50)$$

where $\psi_{p,m}(\tau)$ is the characteristic function of the conditionalized discrete distribution centered at $t = 0$, and is given by

$$\psi_{p,m}(\tau) = \begin{cases} 1, & p = 0 \\ e^{-\frac{i\pi p}{m} \frac{m \sin(\pi p/m)}{\pi} \mathcal{S}_{p,m}}, & p \in \mathbb{Z}_m \setminus \{0\}, \end{cases}, \quad (51)$$

where

$$\mathcal{S}_{p,m} = \frac{\phi_p}{p} + \sum_{l=1}^{\infty} \left(\frac{\phi_{lm+p}}{(lm+p)} - \frac{\phi_{lm-p}}{(lm-p)} \right), \quad p \in \mathbb{Z}_m \setminus \{0\},$$

and ϕ_p is the characteristic function of the pdf g_τ .

From the above theorem, we can write the trigonometric moments for $p \in \mathbb{Z}_m \setminus \{0\}$ as

$$\alpha_{p,m} = E \left[\sin \left(p \frac{2\pi r}{m} \right) \right] = \frac{m \sin(2\pi p/m)}{2\pi} \mathcal{S}_{p,m}, \quad (52)$$

$$\beta_{p,m} = E \left[\cos \left(p \frac{2\pi r}{m} \right) \right] = -\frac{m \sin^2(\pi p/m)}{\pi} \mathcal{S}_{p,m}. \quad (53)$$

An interesting example is the cardioid distribution. The pdf of the cardioid distribution (see Mardia and Jupp 2000, p.45) is given by

$$f(\theta) = \frac{1}{2\pi} (1 + 2\rho \cos(\theta - \mu)), \quad \theta, \mu \in [0, 2\pi), |\rho| < 1/2.$$

Note that ρ is the concentration parameter and $\rho = 0$ gives the circular uniform distribution. The marginalized discrete cardioid distribution will have the probability function

$$p(r|m, \rho, t) = \frac{1}{m} + \frac{2\rho \sin(\pi/m)}{\pi} \cos \left(\frac{2\pi(r - (2t - 1)/2)}{m} \right), \quad r, t \in \mathbb{Z}_m. \quad (54)$$

We note that the probability function (54) is also the conditionalized distribution supported on \mathbb{Z}_m based on cardioid distribution, but with a different concentration parameter $= 2\rho \sin(\pi/m)$ and mean parameter $= \pi(2t - 1)/m$. So, an interesting property of the cardioid distribution is its marginalized discrete distribution is a member of the family of conditionalized discrete distributions. Indeed, this property will hold for infinite mixtures of cardioid distributions as given by the following theorem.

Theorem 5.

Consider the pdf of the parent family defined by

$$f(\theta) = \frac{1}{2\pi} \sum_{k=1}^{\infty} \eta_k (1 + 2\rho_k \cos(\theta - \mu_k)), \quad \theta \in [0, 2\pi), \quad (55)$$

where $\sum_{k=1}^{\infty} \eta_k = 1$, $\forall k$, $\eta_k \geq 0$, $\mu_k \in [0, 2\pi)$, $|\rho_k| < 1/2$. Then the marginalized discrete distribution is also a member of the family of conditionalized discrete distributions.

To visualize marginalized discrete distributions, Figure 2 plots the probability functions on the line for (i) MDVM for $\kappa = 0, 0.5, 1$ and 2.5 and (ii) MDWC for $\rho = 0, 0.25, 0.50$ and 0.75 , with $m = 10$, centered at $t = 5$. We know analytically from Theorem 4 that the marginalized discrete distribution will have two modes, at $t-1$ and t , and the distribution is symmetric about $t - 1/2$, which can be seen in both the graphs (i) and (ii). It can be seen that for small values of the concentration parameters (κ for MDVM and ρ for MDWC) the distribution is diffused and gets more concentrated as concentration parameter increases. We selected $m = 10$ in the

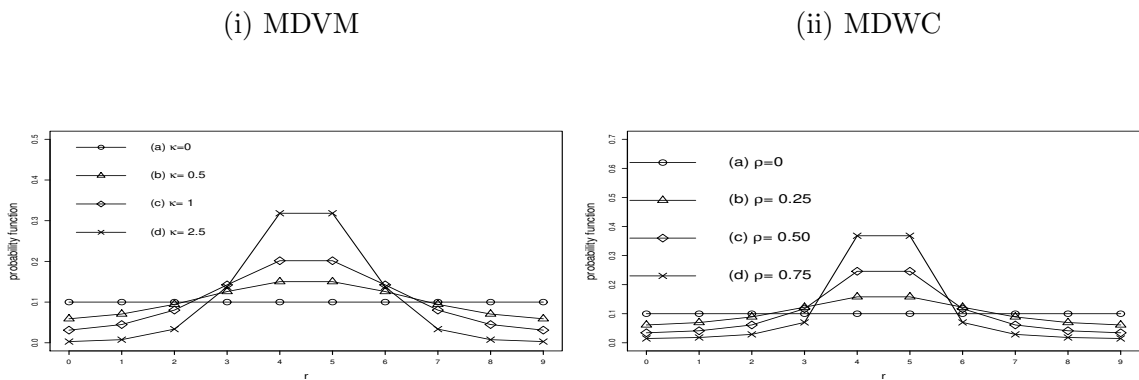


Figure 2: Probability functions of marginalized discrete circular distributions plotted on the line for (i) MDVM for $\kappa = 0, 0.5, 1$ and 2.5 and (ii) MDWC for $\rho = 0, 0.25, 0.50$ and 0.75 , with $m = 10$, centered at $t = 5$.

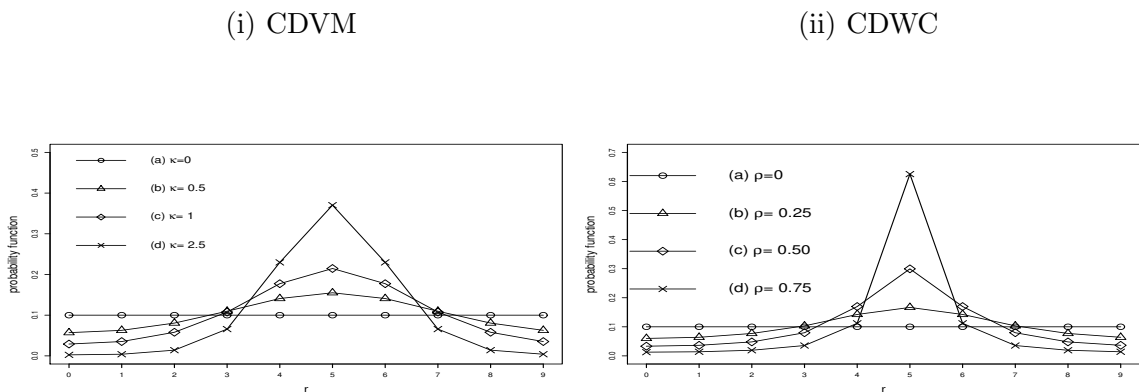


Figure 3: Probability functions of conditionalized discrete circular distributions plotted on the line, with $m = 10$, centered at $t = 5$. (i) CDVM for $\kappa = 0, 0.5, 1$ and 2.5 and (ii) CDWC for $\rho = 0, 0.25, 0.50$ and 0.75 .

figure to also clearly see the difference between marginalized and conditionalized distributions.

The corresponding conditionalized distributions (CDVM and CDWC) are shown in Figure 3. We can see by comparing the two figures that the conditionalized distribution is more peaked than the corresponding marginalized distribution for both von Mises and wrapped Cauchy. We note that for larger m (e.g. $m = 37$ as in roulette wheel data) the marginalized and conditionalized distributions are very close.

Using equation (51), Table 1 shows the characteristic functions for marginalized discrete distributions obtained from von Mises, wrapped Cauchy and cardioid distributions.

Table 1: Characteristic functions of marginalized discrete distributions ($m \geq 2$).

Parent	ϕ_p	$\psi_{p,m}$
Cardioid	$\begin{cases} 1, & p = 0 \\ \rho & p = \pm 1 \end{cases}$	$\begin{cases} 1, & p = 0 \\ e^{-\frac{i\pi}{m} \frac{m\rho \sin(\pi/m)}{\pi}}, & p = 1, m-1 \\ 0, & 2 \leq p \leq m-2. \end{cases}$
von Mises	$\frac{I_p(\kappa)}{I_0(\kappa)}$	$e^{-\frac{i\pi p}{m} \frac{m \sin(\pi p/m)}{\pi I_0(\kappa)}} \left\{ \frac{I_p(\kappa)}{p} + \sum_{l=1}^{\infty} \left(\frac{I_{lm+p}(\kappa)}{(lm+p)} - \frac{I_{lm-p}(\kappa)}{(lm-p)} \right) \right\},$ $0 \leq p \leq m-1.$
wrapped Cauchy	ρ^p	$\begin{cases} 1, & p = 0, \\ e^{-\frac{i\pi p}{m} \frac{m \sin(\pi p/m)}{\pi}} \int_0^{\rho} \frac{x^{p-1}(1-x^{m-2p})}{1-x^m} dx, & 1 \leq p \leq m-1. \end{cases}$

3.2 Properties of the conditionalized discrete distributions

The probability function of the conditionalized discrete distribution based on the circular location family (48) is given by

$$p(r|m, \tau, t) = \frac{g_{\tau}(2\pi(r-t)/m)}{\sum_{r=0}^{m-1} g_{\tau}(2\pi r/m)}. \quad (56)$$

We will call this distribution the “conditionalized discrete circular location family” and summarize its properties in the following theorem.

Theorem 6. *The conditionalized discrete circular location family inherits important properties from (48), namely*

- (a) *It has normalizing constant free of centering parameter t .*
- (b) *It is unimodal and the mode is at $r = t$.*
- (c) *It is symmetrical about t .*

(d) Its characteristic function ((for integer $p \pmod{m}$) is

$$E \left[e^{ip \frac{2\pi r}{m}} \right] = e^{ip \frac{2\pi t}{m}} \psi_{p,m}(\tau), \quad (57)$$

where $\psi_{p,m}(\tau)$ is the characteristic function of the conditionalized discrete distribution centered at $t = 0$, and is given by

$$\psi_{p,m}(\tau) = \frac{\phi_p + \sum_{l=1}^{\infty} (\phi_{lm+p}(\tau) + \phi_{lm-p}(\tau))}{1 + 2 \sum_{l=1}^{\infty} \phi_{lm}(\tau)}, \quad p \in \mathbb{Z}_m. \quad (58)$$

where ϕ_p is the characteristic function of the pdf g_τ .

From the above theorem, the trigonometric moments for $p \in \mathbb{Z}_m \setminus \{0\}$ are

$$\alpha_{p,m} = E \left[\sin \left(p \frac{2\pi r}{m} \right) \right] = 0 \quad \text{and} \quad \beta_{p,m} = E \left[\cos \left(p \frac{2\pi r}{m} \right) \right] = \psi_{p,m}(\tau). \quad (59)$$

Figure 3 plots the probability functions on the line for (i) CDVM for $\kappa = 0, 0.5, 1$ and 2.5 and (ii) CDWC for $\rho = 0, 0.25, 0.50$ and 0.75 , with $m = 10$, centered at $t = 5$. As expected from Theorem 6 the distributions shown in parts (i) and (ii) of the figure are unimodal with mode at t and are symmetric about t . Similar to our observation in the case of marginalized distributions, for small values of the concentration parameters (κ for CDVM and ρ for CDWC) the distribution is diffused and gets more concentrated as concentration parameter increases.

Using equation (58), Table 2 shows the characteristic functions for conditionalized discrete distributions obtained from von Mises, wrapped Cauchy and cardioid distributions.

Table 2: Characteristic functions of conditionalized discrete distributions ($m \geq 2$).

Parent	ϕ_p	$\psi_{p,m}$
Cardioid	$\begin{cases} 1, & p = 0 \\ \rho, & p = \pm 1 \\ 0, & \text{otherwise.} \end{cases}$	$\begin{cases} 1, & p = 0 \\ \rho, & p = 1, m-1 \\ 0, & 2 \leq p \leq m-2 \end{cases}$
von Mises	$\frac{I_p(\kappa)}{I_0(\kappa)}$	$\frac{I_p(\kappa) + \sum_{l=1}^{\infty} (I_{lm+p}(\kappa) + I_{lm-p}(\kappa))}{1 + 2 \sum_{l=1}^{\infty} I_{lm}(\kappa)}, \quad 0 \leq p \leq m-1$
wrapped Cauchy	ρ^p	$\frac{\rho^p (1 + \rho^{m-2p})}{1 + \rho^m}, \quad 0 \leq p \leq m-1$

We now make some additional observations on the CDVM and CDWC distributions.

- (a) For the CDVM distribution, we can also obtain an alternative simplified form for the characteristic function. Let us write

$$L_p(\kappa) = \sum_{r=0}^{m-1} \cos \left(p \frac{2\pi r}{m} \right) e^{\kappa \cos \left(\frac{2\pi r}{m} \right)}. \quad (60)$$

From Theorem 6, we have

$$E \left[e^{ip \frac{2\pi r}{m}} \right] = e^{ip \frac{2\pi t}{m}} B_p(\kappa), \text{ where } B_p(\kappa) = \frac{L_p(\kappa)}{L_0(\kappa)}. \quad (61)$$

$L_p(\kappa)$ behaves like the Bessel function $I_p(\kappa)$; so we have the following identities (Mardia and Jupp 2000, Appendix 1) with $I_p(\kappa)$ replaced by $L_p(\kappa)$.

$$L'_p(\kappa) = \frac{1}{2}(L_{p-1}(\kappa) + L_{p+1}(\kappa)) \text{ and } L'_0(\kappa) = L_1(\kappa), \quad (62)$$

where $L'_p(\kappa) = \frac{dL_p(\kappa)}{d\kappa}$. It then follows by writing $B_1(\kappa) = B(\kappa)$, that

$$B(\kappa) = E \left(\cos \frac{2\pi r}{m} \right) \text{ and } B'(\kappa) = Var \left(\cos \frac{2\pi r}{m} \right). \quad (63)$$

Since for large m CDVM tends to VM, we can show from Mardia and Jupp (2000, Appendix 1 p.349 equation A.4) that we have for large κ and m ,

$$L_p(\kappa) \approx \frac{m}{\sqrt{2\pi\kappa}} e^\kappa. \quad (64)$$

Some Bessel function identities do not hold for the discrete version (see supplement). However, as expected, these identities hold for large m and κ .

- (b) For the CDWC distribution, It follows from Table 2 that the p th trigonometric moments of $CDWC(m, \rho)$ are given by

$$\alpha_{p,m} = E \left[\sin \left(p \frac{2\pi r}{m} \right) \right] = 0, \quad \beta_{p,m} = E \left[\cos \left(p \frac{2\pi r}{m} \right) \right] = \frac{\rho^p (1 + \rho^{m-2p})}{1 + \rho^m}. \quad (65)$$

For $p = 1$, this leads to the mean resultant length

$$\rho_w = \frac{\rho(1 + \rho^{m-2})}{1 + \rho^m}. \quad (66)$$

In general, $0 \leq \rho_w \leq 1$ and as $m \rightarrow \infty$, $\rho_w \rightarrow \rho$. By property of characteristic functions, in general $0 \leq \beta_{p,m} \leq 1$, and as $m \rightarrow \infty$, $\beta_{p,m} \rightarrow \rho^p$, as can be seen from equation (65), thus leading to the characteristic function of the wrapped Cauchy distribution as expected. Further, this convergence happens at an exponential rate. To see this, note that

$$\psi_{p,m}(\rho) - \rho^p = \frac{\rho^p (\rho^{m-2p} - \rho^m)}{1 + \rho^m} = \frac{\rho^{m-p} (1 - \rho^{2p})}{1 + \rho^m}.$$

It follows that $|\psi_{p,m}(\rho) - \rho^p| \leq \rho^{m-p}$, and hence $|\psi_{p,m}(\rho) - \rho^p| = \mathcal{O}(\rho^{m-p})$. In particular, since $\psi_{1,m} = \rho_w$, we have $|\rho_w - \rho| = \mathcal{O}(\rho^{m-1})$ (see supplement for an illustrative plot).

4 Inference: estimation and testing

In this section, we will discuss maximum likelihood estimation and uniformity tests using the marginalized and conditionalized discrete location families of distributions, which were discussed in the previous section.

Suppose $\mathbf{w} = (w_1, w_2, \dots, w_n)$ is an iid sample from a discrete distribution (56) with support \mathbb{Z}_m . Let n_r be the number of data points with $w_i = r$, where $r \in \mathbb{Z}_m$. We will use the following notation for trigonometric moments for discrete data.

$$a_p = \frac{1}{n} \sum_{r=0}^{m-1} n_r \cos\left(p \frac{2\pi r}{m}\right), \quad b_p = \frac{1}{n} \sum_{r=0}^{m-1} n_r \sin\left(p \frac{2\pi r}{m}\right), \quad m'_p = a_p + ib_p = \bar{R}_p e^{i\bar{\theta}_p}, \quad (67)$$

where $\bar{\theta}_p$ and \bar{R}_p denote the p th sample mean direction and p th sample mean resultant length. In particular, for the first trigonometric moments, we will write

$$\bar{C} = \sum_{r=0}^{m-1} \frac{n_r}{n} \cos \frac{2\pi r}{m}, \quad \bar{S} = \sum_{r=0}^{m-1} \frac{n_r}{n} \sin \frac{2\pi r}{m} \quad \text{and} \quad \bar{R} = \sqrt{\bar{C}^2 + \bar{S}^2}. \quad (68)$$

Further, the sample mean direction will be denoted by

$$\bar{\theta} = \tan^{-1} \left(\frac{\bar{S}}{\bar{C}} \right), \quad (69)$$

where $\bar{\theta} \in [0, 2\pi)$ is taken from the appropriate quadrant. We will first discuss the general methodology and then some specific cases of CDVM and CDWC only, where some further simplification in the methodology is possible. We will also consider a nonparametric test (Pearson type chi-square statistic for circular data, i.e. U_G^2 as defined below) for testing uniformity.

4.1 Estimation and testing with discrete circular distributions

The data log-likelihood based on the marginalized discrete probability function (49) can be written as

$$LL(\mathbf{w}|m, \tau, t) = \sum_{r=0}^{m-1} n_r \log \int_{2\pi r/m}^{2\pi(r+1)/m} g_\tau(\theta - 2\pi t/m) d\theta, \quad (70)$$

and the log-likelihood based on the conditionalized discrete probability function (56) can be written as

$$LL(\mathbf{w}|m, \tau, t) = -n \log \left(\sum_{r=0}^{m-1} g_\tau(2\pi r/m) \right) + \sum_{r=0}^{m-1} n_r \log g_\tau(2\pi(r-t)/m). \quad (71)$$

The maximum likelihood estimate (mle) can then be obtained by maximizing $LL(w|m, \tau, t)$ over τ and $t \in \mathbb{Z}_m$. Another problem of interest is to test for uniformity, i.e. testing the hypothesis

$$H_0 : \tau = 0 \text{ vs. } H_1 : \tau \neq 0.$$

We note that under the null hypothesis (H_0), we can assume $t = 0$ without any loss of generality. Here, we describe a testing procedure based on the likelihood ratio statistic. Given the data vector \mathbf{w} of iid observations, we define the test statistic (T) as

$$T(\mathbf{w}, \hat{\tau}, \hat{t}) = -2LL(\mathbf{w}|m, \tau = 0, t = 0) + 2LL(\mathbf{w}|\hat{\tau}, \hat{t}), \quad (72)$$

where $(\hat{\tau}, \hat{t})$ is the mle based on the data vector \mathbf{w} and $LL(\cdot)$ is the log-likelihood as in equation (71). The test rule is to reject H_0 for large values of T or small values of the p-value. If we denote the computed value of T in the data sample by T_d , then

$$\text{p-value} = P(T(\mathbf{w}, \hat{\tau}, \hat{t}) \geq T_d).$$

For a comparison, we will also look at test of uniformity based on the following ‘‘ad hoc’’ test statistics.

(a) Let us consider the circular Karl-Pearson chi-squared statistic (see Mardia and Jupp 2000, p.117)

$$U_G^2 = \frac{1}{nm} \sum_{j=0}^{m-1} \left(S_j - \frac{1}{m} \sum_{i=0}^{m-1} S_i \right)^2, \text{ where } S_j = \sum_{i=0}^j (O_i - E_i), \quad j \in \mathbb{Z}_m,$$

where O_i =observed frequency at angle $2\pi i/m$ for $i \in \mathbb{Z}_m$, $E_i = \frac{1}{m} \times n$. The 5% and 1% critical values for U_G^2 under H_0 can be approximately obtained from Mardia and Jupp (2000, p.104).

(b) $T_1^2 = 2n\bar{R}^2$, which under H_0 , is approximately chi-squared with 2 degrees of freedom. It is used for the unimodal alternatives, namely, the Rayleigh Test.

(c) $T_2^2 = 2n(\bar{R}^2 + \bar{R}_2^2)$, where \bar{R}_2 is obtained similar to \bar{R} in equation (68), but with $4\pi r/m$ used for computation in place of $2\pi r/m$. Under H_0 , T_2^2 is approximately chi-squared with 4 degrees of freedom. The extra term added to T_1^2 allows axial alternatives.

We note that these three test statistics are known in the context of continuous circular data, but we have adapted these to the discrete case. We use parametric bootstrap to compute measures of uncertainty for the mle. Given the circular nature of parameter t , we compute \bar{R} based on bootstrap replications of mle of t as a measure of uncertainty; larger value of \bar{R} implies lesser uncertainty around mle of t and vice-versa. For $\hat{\tau}$, we compute the standard error (SE). We also use bootstrap resampling to compute the p-value under H_0 used for testing (see supplement for details).

We can expect that for any given sample size, the precision of the estimation will be higher for larger values of the concentration parameter τ , and will increase as sample size increases. Similarly, for the hypothesis test of uniformity, for larger τ , non-uniformity can be more easily detected at smaller sample sizes, but for smaller τ , a larger sample size would be needed. We have verified that this is indeed the case based on an analysis of simulated data for CDVM and CDWC, and also that the testing results were consistent for the three alternative tests mentioned above (see supplement). It is also interesting to note that, for CDVM and CDWC, there is an approximate monotonic relationship between T and \bar{R} . However, since this is not an exact relationship the results from tests based on T_1 will not necessarily be same as that based on T (see supplement). We will next concentrate on the specifics of inference only in the case of CDVM and CDWC, where some further simplification is possible.

4.2 Some specifics on inference for CDVM

Suppose $\mathbf{w} = (w_1, w_2, \dots, w_n)$ is a vector of iid observations from $CDVM(m, \kappa, t)$ with known support, i.e. known m . Then the log-likelihood in (71) can be written as

$$LL(\mathbf{w}|m, \kappa, t) = -n \log(L_0(\kappa)) + n\kappa\bar{R} \cos\left(\bar{\theta} - \frac{2\pi t}{m}\right). \quad (73)$$

The mle of t and κ are unique and can be obtained from the following equations.

$$\hat{t} = \arg \max_{t \in \mathcal{S}_t} \cos \left(\bar{\theta} - \frac{2\pi t}{m} \right) = \left[\frac{m\bar{\theta}}{2\pi} \right]_m, \quad (74)$$

$$B(\hat{\kappa}) = \bar{R} \cos \left(\bar{\theta} - \frac{2\pi \hat{t}}{m} \right), \quad (75)$$

where $[x]_m$ denotes the integer closest to the number x , modulo m . Calculation of \hat{t} is direct since $\bar{\theta}$ is easily calculated from the data and we find based on simulations that $2\pi\hat{t}/m$ does not vary much from $\bar{\theta}$ getting closer as n or κ increases (see supplement for a pictorial illustration of (74) and simulation details). By equation (63), $B(\kappa)$ is strictly increasing and therefore for the given \hat{t} , equation (75) can be inverted to get $\hat{\kappa}$.

4.3 Some specifics on inference with CDWC

Suppose $\mathbf{w} = (w_1, w_2, \dots, w_n)$ is a vector of iid observations from $CDWC(m, \rho, t)$ with known support, i.e. known m . Then the log-likelihood in (71) can be written as

$$\begin{aligned} LL(\mathbf{w}|m, \rho, t) &= n (\log(1 - \rho^2) + \log(1 - \rho^m) - \log(m) - \log(1 + \rho^m)) \\ &\quad - \sum_{r=0}^{m-1} n_r \log(1 + \rho^2 - 2\rho \cos(2\pi(r-t)/m)). \end{aligned} \quad (76)$$

The mle is obtained by maximizing $LL(\mathbf{w}|m, \rho, t)$ over $\rho \in [0, 1)$ and $t \in \mathbb{Z}_m$. We note that the likelihood is not necessarily concave (see supplement) but mle can be computed. For any given t , let

$$h(\rho, t) = \frac{1}{n} \frac{\partial LL}{\partial \rho} = -\frac{2\rho}{1 - \rho^2} - \frac{2m\rho^{m-1}}{1 - \rho^{2m}} - \sum_{r=0}^{m-1} \frac{n_r}{n} \frac{2\rho - 2\cos(2\pi(r-t)/m)}{1 + \rho^2 - 2\rho \cos(2\pi(r-t)/m)}. \quad (77)$$

The above expression (for $\rho \neq 0$) can be simplified as

$$h(\rho, t) = -\frac{(1 + \rho^2)}{\rho(1 - \rho^2)} - \frac{2m\rho^{m-1}}{1 - \rho^{2m}} + \frac{1 - \rho^2}{\rho} \sum_{r=0}^{m-1} \frac{n_r}{n} \frac{1}{\rho^2 + 1 - 2\rho \cos \frac{2\pi(r-t)}{m}}. \quad (78)$$

Let

$$\hat{\rho}(t) = \begin{cases} 0, & \text{if } h(\rho, t) < 0 \forall \rho \in [0, 1), \\ 1, & \text{if } h(\rho, t) > 0 \forall \rho \in [0, 1), \\ \tilde{\rho}, & \text{if } h(\tilde{\rho}, t) = 0, \text{ for some } \tilde{\rho} \in [0, 1). \end{cases} \quad (79)$$

The mle for $\hat{\rho}$ is unique if

$$h(\hat{\rho}(t), t) \geq 0 \text{ for } \rho \leq \hat{\rho}(t) \quad \text{and} \quad h(\hat{\rho}(t), t) < 0 \text{ for } \rho > \hat{\rho}(t), \quad \forall t \in \mathbb{Z}_m. \quad (80)$$

Accordingly, the mle $(\hat{t}, \hat{\rho})$ should then satisfy

$$\hat{t} = \arg \max_{t \in \mathcal{S}_t} LL(\mathbf{w}|m, \hat{\rho}(t), t), \quad (81)$$

$$h(\hat{\rho}, \hat{t}) = 0 \text{ except for extreme cases } \hat{\rho} = 0 \text{ or } 1. \quad (82)$$

We conjecture that the mle is unique in general and in fact, it is the case for all the data used in this paper (see supplement for a graphical illustration of how the solution propagates for different values of t).

Due to the closed form expression for trigonometric moments in the case of CDWC, one could consider an alternative estimation approach for estimating ρ . Given the estimate of the centering parameter, we can use the moment estimator of ρ by inverting the function in equation 66, by taking $\hat{\rho}_w = \bar{R}$ (see supplement).

Note that ρ_w gets closer to ρ as $\rho \rightarrow 0$ or $\rho \rightarrow 1$, and this proximity will improve for larger m , indeed $\rho_w \rightarrow \rho$ as $m \rightarrow \infty$. Furthermore, we have shown in Section 3 that CDWC tends to wrapped Cauchy for large m ; so in that case one can estimate the parameters using the maximum likelihood methods for wrapped Cauchy (e.g. using the R routine given in Pewsey et al. (2013) of Kent and Tyler (1988)).

5 Changepoint and Mixtures

Here, we discuss general methodology of changepoint detection and mixtures as motivated by two practical applications, which we are going to apply in the next section. However, we will make specific distributional choices for our data examples and will explain our reasoning fully in sections 6 and 7.

5.1 Changepoint detection

When data is obtained as a sequence of streaming independent observations, it is of interest to estimate components by detecting an appropriate changepoint. Suppose we obtain in a sequence of observations: $\{w_i : i \in \{1, 2, \dots, n\}\}$. Our goal is to estimate a change-point in the data. The model with a changepoint at $i = K$ can be constructed as follows:

$$w_i \sim \begin{cases} p(\cdot|m, \tau_1, t_1) & \text{if } i \leq K \\ p(\cdot|m, \tau_2, t_2) & \text{if } i > K, \end{cases} \quad (83)$$

where $p(\cdot|m, \tau, t)$ is the probability function of the discrete circular distribution as in equations (49) and (56). The likelihood for the data can be written as

$$L(\mathbf{w} | (\tau_1, \tau_2), (t_1, t_2), K) = \prod_{i=1}^K p(w_i | m, \tau_1, t_1) \times \prod_{i=K+1}^n p(w_i | m, \tau_2, t_2). \quad (84)$$

Of particular interest in many applications is to detect a change from uniformity, i.e. $\tau_1 = 0$, where t_1 can be arbitrary but we take as 0 without loss of generality. An example is that of the gaming roulette, where the casino is interested in detecting a deviation from the uniform distribution as early as possible based on sequence of roulette spins. We can use Bayesian estimation with non-informative flat priors on the unknown parameters, viz τ_1, t_1, τ_2, t_2 and K . Suppose this prior is denoted by $\pi(\tau_1, \tau_2, t_1, t_2, K)$, then the joint posterior distribution is obtained as

$$\Pi((\tau_1, \tau_2, t_1, t_2, K) | \mathbf{w}) \propto L(\mathbf{w} | (\tau_1, \tau_2), (t_1, t_2), K) \times \pi(\tau_1, \tau_2, t_1, t_2, K). \quad (85)$$

Gibbs sampling can be used to simulate from the posterior distribution of the parameters and then generate the relevant summaries (see supplement for computational steps and a test

example). Pewsey and García-Portugués (2020) have given a survey of changepoint detection with continuous angular data, but our method is for circular data, which is discrete.

5.2 Discrete circular mixtures

We now consider constructing mixture of discrete circular distribution components. The probability function for a mixture of K distribution components can be written as

$$p(r|m, (\tau_1, \dots, \tau_K), (t_1, \dots, t_K)) = \sum_{j=1}^K p_j \cdot p(r|m, \tau_j, t_j), \quad (86)$$

where p_j is the mixing probability, τ_j and t_j are the concentration and centering parameters of the j^{th} discrete distribution component. Note that this K is not to be confused with the notation for changepoint used in the last subsection. Suppose we have $\mathbf{w} = (w_1, w_2, \dots, w_n)$ a vector of iid observations from a discrete distribution mixture with a known number of components K . We would be interested in estimating the component-wise parameters (τ_j, t_j) and also the corresponding mixing probabilities p_j . The likelihood for the data can be written as

$$L(\mathbf{w}|m, \boldsymbol{\tau}, \mathbf{t}, \mathbf{p}) = \prod_{i=1}^n p(w_i|m, (\tau_1, \dots, \tau_K), (t_1, \dots, t_K)). \quad (87)$$

We use Bayesian estimation with non-informative flat priors on the parameters $\boldsymbol{\tau} = (\tau_1, \dots, \tau_K)$, $\mathbf{t} = (t_1, \dots, t_K)$ and the mixing probabilities $\mathbf{p} = (p_1, \dots, p_K)$, and obtain their posterior distribution conditional on the data. Suppose this prior is denoted by $\pi(\boldsymbol{\tau}, \mathbf{t}, \mathbf{p})$, then the joint posterior distribution is obtained as

$$\Pi(\boldsymbol{\tau}, \mathbf{t}, \mathbf{p}|\mathbf{w}) \propto L(\mathbf{w}|m, \boldsymbol{\tau}, \mathbf{t}, \mathbf{p}) \times \pi(\boldsymbol{\tau}, \mathbf{t}, \mathbf{p}). \quad (88)$$

Gibbs sampling can be used to simulate from the posterior distribution of the parameters and then generate the relevant summaries (see supplement for computational steps and a test example).

6 Examples

Using the methods developed in the previous sections, we analyse real data examples of the online as well as casino roulette wheel data, and smart home eating habit human eating activity data.

6.1 Roulette data: online gaming and casino spins

There has been ongoing search to find a plausible test for testing unbiasedness of a roulette wheel. We described the roulette example in the introduction section and the need of suitable test for bias as well as detection of changepoint when bias creeps in. The problem is now more pressing than ever before with the rise of many online gaming sites, e.g. https://10bestcasinos.co.uk/en-en_d_r1.html. Indeed, Mardia (1972, p. 50), has touched the problem and proposed two simple models: we have already described the model based on the geometric model in Section 2. He also proposed

$$P(\theta = 0) = c_2 p, P(\theta = 2\pi|r|/m) = c_2 p/|r|, |r| = 1, \dots, n,$$

where c_1 and c_2 are the normalizing constants. But these distributions are of course not as flexible as our proposed families and were not applied. To illustrate our procedure, we consider data sequences obtained from spins of three different European roulette wheels. Note that here $m = 37$ (as against American roulette $m = 38$).

Data 1 Our first data is of size $n = 1000$, a sequence of outcomes from successive spins of an online European roulette simulator.

Data 2 This data has outcome from successive spins of a real European roulette recorded in a casino.

Data 3 This data is from the same casino as Data 2, but from a different roulette wheel.

Data 1, 2 and 3 are of size $n = 1000, 8299$ and 8106 respectively (see supplement for their frequency distribution tables). The main challenge is to detect a possible bias in a roulette based on its data sequence. We note here that since the roulette data is a time series, we have done a test of serial independence, which indicates overall there is no dependence (see Section 6.1.1). We consider different types of analysis as described below.

Analysis 1 : Bias testing (Section 4)

Analysis 2 : Changepoint detection based on full data sequence as well as partial data sequences (Section 5.1), and

Analysis 3 : Two-component mixture where one component is forced to uniform and the other is estimated along with its mixing probability (Section 5.2).

We carry out these analyses with the following model choices. For Analysis 1, we show results from both CDVM and CDWC, but for Analyses 2 and 3, we will just present results for CDWC, as the results would be similar under either distribution.

Analysis 1 After mapping the roulette outcome to the corresponding angle position (w), we applied the estimation and testing procedure described in Section 4. Table 3 shows the computations of mle and the test statistics T based on CDVM as well as CDWC along with p-value to test

$$H_0 : \text{unbiased wheel vs. } H_1 : \text{biased wheel.}$$

The estimated value of the concentration parameter κ being slightly different from 0 is a preliminary indication of a biased wheel. However, we further carry out a formal test to check statistical significance based on the statistic T as in Section 4. The larger p-value (0.715) for Data 1 suggests that there is not much evidence to indicate the wheel is biased. The p-value for Data 2 (0.039) is below 5% significance level but above 1% suggesting that there is weak evidence for a biased wheel. For Data 3, a small p-value clearly suggests evidence for a biased wheel. We note in general that the mle for the t parameter for a roulette need not coincide with the mode of the frequency distribution (e.g. for Data 1, $\hat{t} = 17$ but mode of the frequency distribution is 0). This is because the value of t for which the CDVM likelihood is maximized also depends on value of κ .

For a comparison, we also carried out alternative tests based on the statistics U_G^2 , T_1^2 and T_2^2 as described in Section 4 (see supplement). It is satisfying to note that these results are mostly consistent with the above observations made from Table 3. Incidentally, we note in

Table 3: For CDVM and CDWC, results of mle and statistical testing for bias based on the test statistic T , for the 3 European roulettes. For both CDVM and CDWC, the p-value suggests no evidence for bias in Data1, weak evidence for Data 2 and strong evidence for bias in Data3.

(a) CDVM

	roulette	n	\bar{R}	$\hat{\kappa}$	SE($\hat{\kappa}$)	\hat{t}	$\hat{\theta} = \frac{2\pi\hat{t}}{m}$	$\bar{R}(\hat{\theta})$	T	SE(T)	p-value
(i)	Data 1	1000	0.018	0.036	1.357	17	2.887	1.000	0.654	56.239	0.715
(ii)	Data 2	8299	0.020	0.040	0.567	30	5.094	1.000	6.688	129.634	0.039
(iii)	Data 3	8106	0.029	0.058	0.585	31	5.264	1.000	13.716	130.800	0.001

(b) CDWC

	roulette	n	\bar{R}	$\hat{\rho}$	SE($\hat{\rho}$)	\hat{t}	$\hat{\theta} = \frac{2\pi\hat{t}}{m}$	$\bar{R}(\hat{\theta})$	T	SE(T)	p-value
(i)	Data 1	1000	0.018	0.019	0.018	18	3.057	0.624	0.683	3.228	0.7150
(ii)	Data 2	8299	0.020	0.020	0.007	30	5.094	0.956	6.675	7.128	0.0430
(iii)	Data 3	8106	0.029	0.030	0.008	31	5.264	0.950	14.245	7.098	0.0020

Table 3 part (a) for CDVM (findings are similar for (b) CDWC) that the highest value of \bar{R} is 0.029, and using the mapping between \bar{R} and κ in Mardia and Jupp (2000, Appendix 2.4), we get $\hat{\kappa} = 0.058$, which is same as the mle $\hat{\kappa}$ we obtained for CDVM.

Analysis 2 We apply the approach discussed in 5.1 for changepoint detection using CDWC. For this analysis, recall that the first component before the changepoint is forced to be uniform (i.e. $\rho = 0, t = 0$). We first carry out the analysis based on the full data sequence. The resulting posterior distribution summaries for the three data are shown in Table 4. For Data 1 and Data 2, we do not detect any changepoint as the 95% credible interval for the possible changepoint K is very wide spanning almost over the entire range, with posterior mode close to the extreme. Also, the 95% credible interval is not removed away from 0, suggesting that the second component may not be different from uniform. For Data 3, a changepoint is detected with a likely position being 1997 as indicated by the mode in the posterior distribution of K and also the much narrower 95% credible interval compared to full range of possibilities, and the 95% credible interval for ρ of second component is clearly removed from 0. These findings are consistent with the results of Analysis 1, where Data 3 showed strong evidence for bias. Here, we have gone one step further and determined the likely time-point in the data sequence when the bias may have set in.

Table 4: : Results showing posterior distribution summaries for the distribution after changepoint using CDWC based on full data range for the three roulette data.

	roulette	ρ_2			$2\pi t_2/m$		K		
		mean	sd	95% interval	mean	\bar{R}	mode	sd	95% interval
(i)	Data 1	0.064	0.109	[0 , 0.400]	2.605	0.146	998	305	[42 , 997]
(ii)	Data 2	0.026	0.063	[0 , 0.100]	5.347	0.635	176	2,635	[139 , 8234]
(iii)	Data 3	0.035	0.010	[0.010 , 0.050]	5.295	0.951	1,997	869	[183 , 3414]

Analysis with streaming data: Further, to see how early we can detect a change with

streaming data, we applied the changepoint detection procedure on partial data sequences of the three roulette datasets, i.e. spins $1 : u$ for different bounds u , namely,

$$u \in \{100, 200, \dots, 1000\} \text{ for Data 1 ,}$$

$$u \in \{500, 1000, 1500, \dots, 8000, 8299\} \text{ for Data 2 ,}$$

$$\text{and } u \in \{500, 1000, 1500, \dots, 8106\} \text{ for Data 3.}$$

Figure 4 obtained for Data 1, 2 and 3 shows the plots of the 95% credible intervals, and posterior mean for ρ_2 and mode for K for different choices of the upper bound. For Data 1 and Data 2, we can see that the 95% credible interval for K almost spans across the full range of possibilities, i.e. from 1 to the upper bound of the sequence. Also, the 95% credible intervals for ρ_2 always contain 0 suggesting that the second component may not be different from uniform. For Data 3, we can see that starting from an upper bound of 4500 onwards, the 95% credible interval for K starts becoming much narrower compared to the range of possibilities. Also, correspondingly the 95% credible interval for ρ_2 is clearly removed from 0, and the posterior mode is settled around 2000. So, for Data 3, while we start detecting the change weakly based on data range 1:2500, the evidence becomes stronger starting from 1:4500. In the plot for Data 2, we note that there are a few instances at the right extreme where the mode for K is not close to the upper end of the 95% credible interval. This is due to presence of multiple modes in the posterior distribution based on MCMC simulations, which appear as rapid fluctuations in the dotted line. Given that the posterior is diffused and the 95% credible interval for changepoint spans over almost entire range of possibilities, these modes do not have any significance. In fact, the posterior distribution for Data 2 based on the full data range shows a mode at either extreme (see supplement).

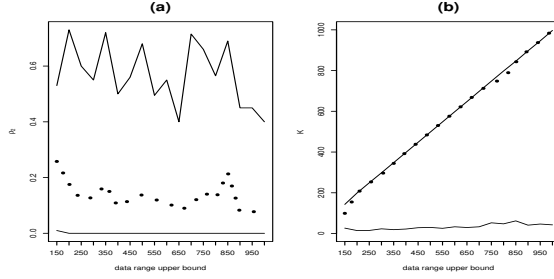
Analysis 3 . We use the procedure described in Section 5.2 on fitting mixture of CDWC components. Table 5 shows the posterior summaries from fitting 2-component CDWC mixture to the three roulette datasets (see supplement for the the posterior distribution plots). For Data 1, it is interesting to note that the 95% credible interval is removed from 0, although the span of the interval is very large (0.01 to 0.91). This suggests that there may be some bias although the evidence for this is again very weak. We recall that the changepoint analysis did not reveal a possible change in the data generating mechanism over time. For Data 2, the 95% credible interval for ρ_2 is not removed from 0 suggesting that the second component may not be different from uniform. This finding is again consistent with the changepoint analysis and the testing. For Data 3, the 95% credible interval for ρ_2 is very clearly removed from 0, which is suggestive of a second non-uniform component. This also is consistent with our findings from testing as well as changepoint analysis (Analysis 2).

6.1.1 Test of serial dependence

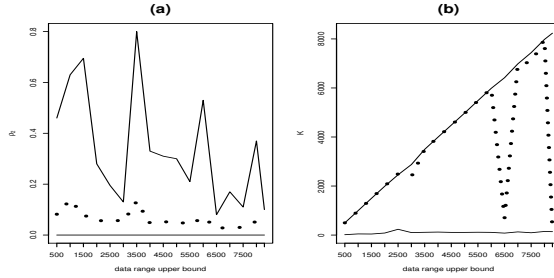
Since the roulette data is a time series data, it is important to assess whether there is any dependence before we apply any iid statistical work. One of the common method of assessing dependence is to use Watson and Beran (1967) serial correlation coefficient to check whether there is presence of first order serial dependence in the three roulette data. Recall $m = 37$ and each roulette outcome $w \in \mathbb{Z}_m$. We consider the sequence of roulette outcomes w_1, w_2, \dots, w_n and compute the following Watson-Beran's modified test, statistics

$$\bar{C} = \frac{1}{n} \sum_{i=2}^n \cos(2\pi(r_i - r_{i-1})/m), \quad \bar{S} = \frac{1}{n} \sum_{i=2}^n \sin(2\pi(r_i - r_{i-1})/m), \quad \bar{R}^2 = \bar{C}^2 + \bar{S}^2,$$

(i) Data 1



(ii) Data 2



(iii) Data 3

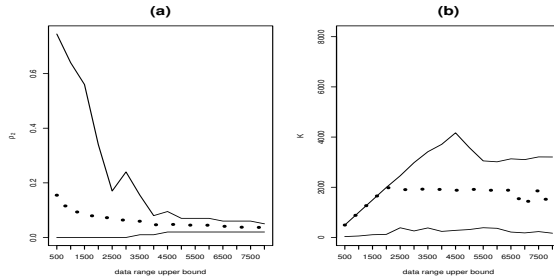


Figure 4: Results of changepoint analysis based on different partial data ranges for Data 1, 2 and 3 shown in rows (i), (ii) and (iii) respectively. Each row of plots shows posterior summaries for ρ_2 and K plotted against data range upper bound, shown as plots (a) and (b) respectively. In each plot, solid lines mark the 95% credible intervals. The dotted line in plot (a) shows the posterior mean for ρ_2 and in plot (b) shows the posterior mode for K .

and we reject the hypothesis of independence at 1% level based on large (absolute) values of the three statistics, though \bar{R} is the omnibus statistic. The required critical values are computed using simulations from the null distribution. We note that for large n and m , the statistics have the following asymptotic null distributions.

$$\sqrt{2n}\bar{C} \sim N(0, 1), \quad \sqrt{2n}\bar{S} \sim N(0, 1) \quad 2n\bar{R}^2 \sim \chi^2(2). \quad (89)$$

Table 6 shows the computed values of the statistics (89) for the three roulette data and the applicable 1% cutoffs calculated based on (100,000) simulations from the null distribution, i.e. discrete circular uniform supported on equi-spaced lattice with $m = 37$ points. We see that for all the three data the statistic values are well within the cutoffs. So, there is no evidence to support existence of serial dependence in any of the roulette sequences. We note that for

Table 5: Results of fitting a 2-component CDWC mixture to the three roulette datasets, with first component forced to uniform (i.e. $\rho_1 = 0, t_1 = 0$). Posterior summaries are shown for the parameters (ρ_2, t_2, p_2) of the second component in the mixture.

(i) Data 1				
	parameter	mean	sd	95% interval
(a)	ρ_2	0.370	0.268	[0.010 , 0.910]
(b)	$2\pi t_2/m$	3.494	0.299	
(c)	p_2	0.070	0.065	[0.003 , 0.296]
(ii) Data 2				
	parameter	mean	sd	95% interval
(a)	ρ_2	0.026	0.014	[0 , 0.050]
(b)	$2\pi t_2/m$	5.087	0.825	
(c)	p_2	0.680	0.103	[0.487 , 0.871]
(iii) Data 3				
	parameter	mean	sd	95% interval
(a)	ρ_2	0.571	0.147	[0.260 , 0.830]
(b)	$2\pi t_2/m$	5.246	0.990	
(c)	p_2	0.062	0.026	[0.026 , 0.126]

the continuous case, the critical values in Table 6 are roughly comparable to that based on the asymptotic distribution (89).

Table 6: Computed statistic values for the three roulette data and the 1% critical value calculated based on (100000) simulations from the null distribution.

		computed statistic values			1% critical value		
roulette	n	$\sqrt{2n\bar{C}}$	$\sqrt{2n\bar{S}}$	$2n\bar{R}^2$	$\sqrt{2n\bar{C}}$	$\sqrt{2n\bar{S}}$	$2L\bar{R}^2$
Data 1	1000	0.436	-0.904	1.007	± 2.574	± 2.576	9.254
Data 2	8299	1.289	-0.314	1.759	± 2.555	± 2.579	9.210
Data 3	8106	-1.697	-0.479	3.110	± 2.569	± 2.580	9.251

6.2 Smart Home and Eating Activity Data

In this section, we study the data taken from CHAD on eating habit activity of a household over a period of about one year recorded at half-hour intervals during the day, hence $m = 48$. The context of the data was described in the introduction section. Figure 5 shows the histogram on the line and the circular histogram for the data. The histogram clearly shows three modes and hence we fit the data with a mixture of 3 components using the Bayesian procedure described in Section 5.2. Since the eating activity data is aggregated data, ideally it is more appropriate to use the marginalized discrete distributions as components rather than conditionalized discrete distributions. However, as we discuss in Section 7, with $m = 48$, the two approaches are expected to give similar results. We fit the data with 3 components of MDWC as well as CDWC.

Table 7 shows posterior summaries for the parameters of a 3-component mixture fitted to the data based on MDWC (part (a)) and CDWC (part (b)). We note the results from the two distributions are similar. The posterior mean values of (t_1, t_2, t_3) are $(14.7, 24.7, 36.5)$ for MDWC and $(14.6, 24.8, 36.2)$ for CDWC. This means that the data is a mixture of three

components approximately centered at 7:30 hours (Breakfast), 12:30 hours (Lunch), and 18:00 hours (Dinner), which is what can be expected for a typical household. Due to the circular nature of the parameters (t_1, t_2, t_3) , we report \bar{R} as a measure of variation and do not compute the credible intervals. Our analysis for this data shows there is relatively more variation in the lunch time for this household as indicated by the smaller \bar{R} corresponding to the second component.

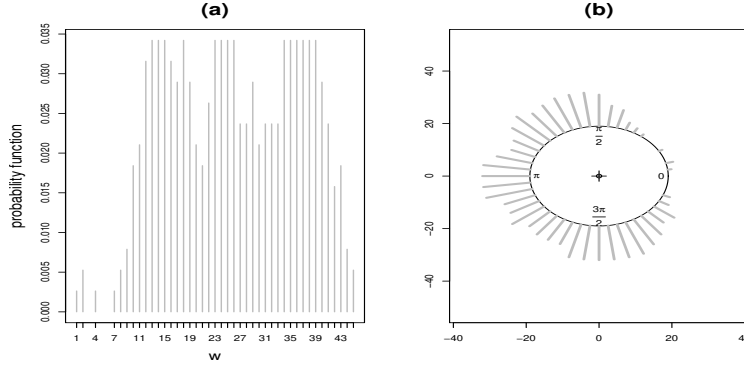


Figure 5: Histogram on the line and circular histogram for the human eating activity data

Table 7: Posterior summaries for the parameters of a 3-component mixture of MDWC (a) and CDWC (b) are shown for the Eating Activity data. The components are shown in the order of increasing estimated centering parameter t .

(a) MDWC					(b) CDWC				
parameter	mean	sd(or $\bar{R}(2\pi t_j/m)$)	95% interval		parameter	mean	sd(or $\bar{R}(2\pi t_j/m)$)	95% interval	
ρ_1	0.731	0.042	0.650	0.815	ρ_1	0.665	0.039	0.580	0.740
ρ_2	0.563	0.058	0.440	0.660	ρ_2	0.562	0.059	0.435	0.660
ρ_3	0.661	0.040	0.580	0.740	ρ_3	0.706	0.036	0.635	0.770
$2\pi/mt_1$	1.969	0.997			$2\pi/mt_1$	1.964	0.996		
$2\pi/mt_2$	3.301	0.993			$2\pi/mt_2$	3.321	0.992		
$2\pi/mt_3$	4.877	0.997			$2\pi/mt_3$	4.845	0.997		
p_1	0.258	0.047	0.160	0.347	p_1	0.300	0.049	0.200	0.395
p_2	0.393	0.068	0.277	0.544	p_2	0.385	0.066	0.267	0.523
p_3	0.349	0.048	0.248	0.439	p_3	0.314	0.046	0.222	0.403

7 Comparisons

In this section, we carry out several comparisons to gain some insights on the choices between the families resulting from marginalized and conditionalized methods, or choices between candidates within a given type of family. We briefly summarize the type of comparisons as follows:

- Cross comparison, i.e. continuous versus discrete models: This is to study the effect on inference if we used the continuous distribution instead of a discrete distribution.

We find that the inference using a continuous model can be misleading especially when we are estimating parameters from discrete data with higher concentration parameter. However, for testing uniformity on highly dispersed data, the use of test based on discrete distribution and the Rayleigh test based on continuous distribution will lead to similar conclusions.

- Comparison within a particular family of discrete distributions, e.g. among conditionalized discrete distributions using on divergence measures: By using Kullback-Leibler, L_1 and L_2 measures, we will show here that the conditionalized discrete distributions resulting from von Mises and wrapped Cauchy can be very different from each other; so one cannot be easily approximated by the other family. In contrast, we show that the conditionalized discrete wrapped normal (defined in Section 7.2) and CDVM are very close to each other; so for practical purposes may be interchangeable in data analysis
- Comparison among different types of discrete models, i.e. marginalized and conditionalized: We note here that except for very small values of m such as $m < 10$, inference based on the marginalized and conditionalized approaches will be similar.
- Re-examination of Sheppard correction for circular distribution directly based on marginalized and conditionalized discrete distributions.

7.1 Comparison of continuous with discrete models: effect on inference

The question is whether using a discrete distribution is really necessary for inference with discrete circular data. The question is whether we would reach similar conclusions if we just carried out the inference based on the approximate continuous model instead of the discrete model. To check this, we study the effect on inference, namely maximum likelihood estimation and testing using simulated data arising from CDVM and CDWC. We expect similar findings to hold for marginalized discrete distributions. We show below that the inference using a continuous model can be misleading especially when we are estimating parameters from discrete data with higher concentration parameter. Also for example when we are dealing with changepoint analysis for roulette data, it is natural to work on discrete support. However, for testing uniformity on highly dispersed data, the use of test based on discrete distribution and the Rayleigh test based on continuous distribution will lead to similar conclusions.

7.1.1 Effect on estimation

We simulate 1000 datasets, each of size $n = 1000$ for each choice of $m \in \{10, 20\}$ and $\kappa \in \{1, 2.5, 10\}$ for $CDVM(m, \kappa, t = 0)$, and $\rho \in \{0.5, 0.6, 0.8\}$ for $CDWC(m, \rho, t = 0)$. We compute the mle from the conditionalized discrete model and compare it with that obtained from the continuous model. Table 8 shows the comparison of bias, standard deviation(sd) and mean squared error (mse)calculated based on the 1000 simulated datasets under different scenarios of m and the concentration parameter (κ or ρ). Part (a) of the table compares CDVM with VM, and part (b) compares CDWC with WC. We used the ‘‘CircStats’’ library in R to compute the mle under von Mises and wrapped Cauchy models.

In part (a) of Table 8 we can see that for $m = 10$, the bias, sd and mse for CDVM are comparable with that of VM for $\kappa = 1, 2.5$, but has lesser bias and mse than that of VM for $\kappa = 10$. However, as m increases to 20, the differences between *CDVM* and *VM* decrease.

In part (b) of Table 8, the differences are more pronounced. For $m = 10$, we see that the bias, sd and mse for CDWC are comparable with that of WC for $\rho = 0.5$, but bias, sd and mse are much lesser than that of *WC* for $\rho = 0.6$ and 0.8 . With increasing m to 20, the differences at $\rho = .6$ decrease but continue to remain at $\rho = 0.8$ indicating that a larger m would be required for the two to match.

In summary, using the continuous model for discrete data with possibly high concentration and moderate m can lead to highly biased and inaccurate estimation of parameters. Further, how large m needs to be for a continuous approximation to work depends on the concentration parameter. In problems, such as in mixture estimation, where the underlying nature of concentration parameters are apriori unknown, it is therefore more appropriate to work with the discrete distribution, as inferences from (the approximate) continuous model can be misleading, i.e. biased with higher standard deviation.

(a) MLE : CDVM vs. VM								(b) MLE : CDWC vs. WC							
m	κ	CDVM			VM			m	ρ	PDWC			WC		
		Bias	SD	MSE	Bias	SD	MSE			Bias	SD	MSE	Bias	SD	MSE
10	1	0.004	0.055	0.055	0.002	0.053	0.053	10	0.5	0.001	0.016	0.016	0.013	0.019	0.023
10	2.5	0.002	0.092	0.092	-0.003	0.092	0.092	10	0.6	-0.000	0.013	0.013	0.058	0.024	0.063
10	10	0.008	0.385	0.385	1.513	0.690	1.663	10	0.8	-0.000	0.007	0.007	*0.200	0.000	0.200
20	1	0.000	0.052	0.052	-0.002	0.051	0.051	20	0.5	-0.001	0.017	0.017	-0.000	0.017	0.017
20	2.5	0.005	0.095	0.095	-0.000	0.094	0.094	20	0.6	0.000	0.014	0.014	0.001	0.014	0.014
20	10	0.035	0.432	0.433	0.042	0.433	0.435	20	0.8	-0.000	0.007	0.007	0.063	0.020	0.066

* mle using `mle.wrappedcauchy()` in R converged to $\rho = 1$ for this case

Table 8: Bias , sd and mse for the mle for the concentration parameter (κ in (a), ρ in (b)) computed based on 1000 datasets, each of size $n = 1000$ for each choice of $m \in \{10, 20\}$ and $\kappa \in \{1, 2.5, 10\}$ for *CDVM*($m, \kappa, t = 0$), and $\rho \in \{0.5, 0.6, 0.8\}$ for *CDWC*($m, \rho, t = 0$).

7.1.2 Effect on test of uniformity

Recall that the test of uniformity for a discrete location family (56) is formulated as $H_0 : \tau = 0$ vs. $H_1 : \tau \neq 0$, where $\tau = \kappa$ for CDVM and $\tau = \rho$ for CDWC. This can be tested based on the discrete distribution using the test statistic T as discussed in Section 4 or an alternative approach is to use the Rayleigh test based on test statistic \bar{R} . Table 9 shows the power computed for a 5% test based on either statistic at a specific alternative, viz. $\kappa = 0.05$ for CDVM and $\rho = 0.03$ for CDWC, for each of different choices of data-size $n \in \{1000, 10000\}$ and $m \in \{10, 37\}$. The 5% critical values and the power for T are computed based 10000 simulated datasets under the null and alternative hypothesis respectively, from the conditionalized discrete distribution (CDVM in (a) and CDWC in (b) with a given value of m) of the given data-size n . The 5% critical values and the power for \bar{R} are computed based 10000 simulated datasets under the null and alternative hypothesis respectively, from the continuous distribution (VM in (a) and WC in (b)) of the given data-size n . For both CDVM and CDWC, we find that the power of the test based on T is comparable to that based on \bar{R} (i.e Rayleigh).

(a) CDVM: $H_0 : \kappa = 0 \quad H_1 : \kappa \neq 0$

n	m	power for 5% test at $\kappa = 0.05$	
		T	Rayleigh (\bar{R})
1000	10	0.1445	0.1606
1000	37	0.1637	0.1668
10000	10	0.8976	0.8967
10000	37	0.8997	0.8992

(b) CDWC: $H_0 : \rho = 0 \quad H_1 : \rho \neq 0$

n	m	power for 5% test at $\rho = 0.03$	
		T	Rayleigh (\bar{R})
1000	10	0.207	0.212
1000	37	0.214	0.209
10000	10	0.974	0.976
10000	37	0.976	0.976

Table 9: shows the power computed for a 5% test based on the statistics T and \bar{R} at a specific alternative, viz. $\kappa = 0.05$ for CDVM and $\rho = 0.03$ for CDWC, for each of different choices of data-size $n \in \{1000, 10000\}$ and $m \in \{10, 37\}$. The 5% critical values and the power for T are computed based 10000 simulated datasets under the null and alternative hypothesis respectively.

7.2 Comparison among discrete distributions based on divergence measures

We will show here that the conditionalized discrete distributions resulting from von Mises and wrapped Cauchy can be very different from each other; so one cannot be easily approximated by the other family. In contrast, we show that the conditionalized discrete wrapped normal (CDWN) and conditionalized discrete von Mises are very close to each other; so for practical purposes may be interchangeable in data analysis.

In order to compare the probability functions of $CDWC(m, \rho, t)$ and $CDVM(m, \kappa, t)$, we need to first map the parameters ρ to κ . We do so by matching their first trigonometric moments given by equations (63) and (66), i.e. $B(\kappa) = \rho_w$. Figure 6 plots the probability functions for (i) $m = 10$ and (ii) $m = 37$ with $t = 5$ and $t = 16$ respectively, for $\rho = 0.5$ and its mapped κ value. We see that the CDWC is more spiked and heavy tailed compared to CDVM.

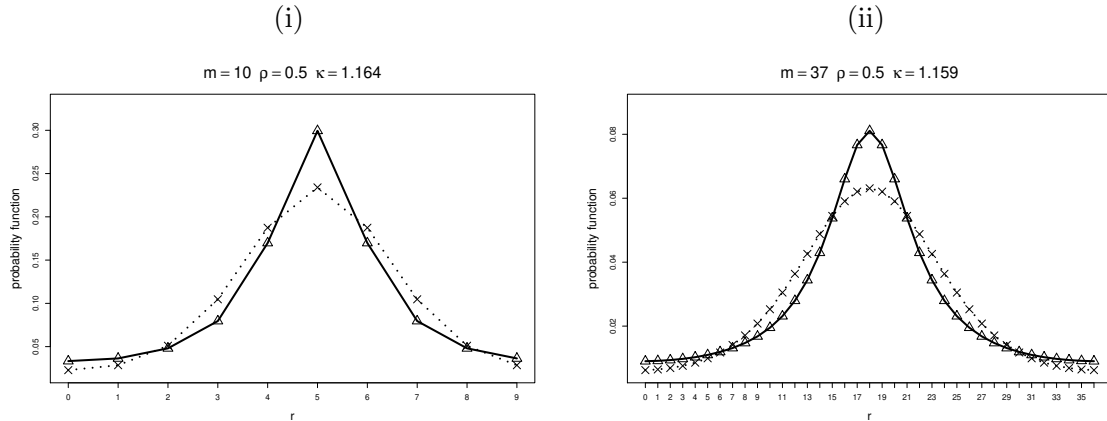


Figure 6: Probability functions of $CDWC(m, \rho, t)$ (triangles joined by solid line) and $CDVM(m, \kappa, t)$ (cross joined by dotted lines) plotted for (i) $m = 10$ and (ii) $m = 37$ with $t = 5$ and $t = 16$ respectively, for $\rho = 0.5$ and its mapped κ value by matching the first trigonometric moment.

Further, to assess the differences quantitatively, we compute the maximum possible dis-

tance between CDVM and CDWC using the Kullback-Leibler divergence (KL), L_1 and L_2 norms. Suppose f_1, f_2 are members of the circular location family (48) with mode at 0, and \tilde{p}_1, \tilde{p}_2 be the respective conditionalized discrete distributions supported on $\{2\pi r/m, r \in \mathbb{Z}_m\}$. For our purpose, \tilde{p}_1, \tilde{p}_2 are members of the conditionalized discrete location family. Then we define

$$KL(\tilde{p}_1, \tilde{p}_2) = \sum_{r=0}^{m-1} \tilde{p}_1(2\pi r/m) \log \frac{\tilde{p}_1(2\pi r/m)}{\tilde{p}_2(2\pi r/m)}. \quad (90)$$

$$L_1(\tilde{p}_1, \tilde{p}_2) = \sum_{r=0}^{m-1} |\tilde{p}_1(2\pi r/m) - \tilde{p}_2(2\pi r/m)|. \quad (91)$$

$$L_2(\tilde{p}_1, \tilde{p}_2) = \sqrt{\sum_{r=0}^{m-1} (\tilde{p}_1(2\pi r/m) - \tilde{p}_2(2\pi r/m))^2} \times \frac{m}{2\pi}. \quad (92)$$

We include the constant factor $m/(2\pi)$ in the definition of discrete L_2 norm to ensure that it matches the L_2 norm of the continuous case as m tends to infinity. So, we have

$$\lim_{m \rightarrow \infty} KL(\tilde{p}_1, \tilde{p}_2) = KL(f_1, f_2), \lim_{m \rightarrow \infty} L_1(\tilde{p}_1, \tilde{p}_2) = L_1(f_1, f_2), \lim_{m \rightarrow \infty} L_2(\tilde{p}_1, \tilde{p}_2) = L_2(f_1, f_2). \quad (93)$$

For CDWC with respect to CDVM (as base), Table 10 (a) shows the maximum values for KL , L_1 and L_2 for $m = 10, 37, 1000$ and 10000 , and the maximizing values of ρ_w . We emphasize that for $m = 1000$ and $m = 10000$, the maximum KL , L_1 and L_2 may be attained at values larger than $\rho_w = 0.995$, but have not been computed due to numerical computational issues with larger ρ_w . We also see that as m increases the maximum KL , and the ρ_w at which it is attained also increases. As a yard stick reference for analysing, we also compute KL , L_1 and L_2 for the conditionalized discrete wrapped normal (CDWN) distribution with base as CDVM, again by mapping the parameters based on first trigonometric moments. The CDWN can be constructed starting from the wrapped normal using the approach given in Section 2, equation (29), and its probability function can be shown to be

$$p(r|m, \rho, t) = \frac{1 + 2 \sum_{q=1}^{\infty} \left[\rho^{q^2} \cos\{q(2\pi(r-t)/m)\} \right]}{m \left(1 + 2 \sum_{k=1}^{\infty} \rho^{k^2 m^2} \right)}, \quad r, t \in \mathbb{Z}_m, \rho \in [0, 1), \quad (94)$$

where ρ is the mean resultant length parameter of the wrapped normal (WN). In fact, this is a particular case of conditionalized discrete wrapped stable distributions, which we discuss in Section 8.4.

Table 10 (b) shows the results for CDWN versus CDVM. Pewsey and Jones (2005) have observed that the von Mises and wrapped normal distributions are very close with respect to L_1 and L_2 norms. Our findings in Table 10 (b) are consistent with their work, in that the L_1 and L_2 values we compute for large m ($m=10000$) closely match their computations. Further, we can see from Table 10 that CDWN and CDVM are much closer with respect to KL , L_1 and L_2 than CDWC and CDVM. So, in general, CDWC is very different from CDVM. However, CDVM and CDWC can be close for small values of ρ (e.g. $\rho < 0.1$), but are not so for larger ρ due to the heavy tail nature of CDWC (see supplement). Further, for $m \rightarrow \infty$, the CDVM becomes VM, CDWC becomes WC and CDWN become WN. The following result shows that the maximum KL of WC with base as VM is infinite, whereas the KL of WN with base as VM goes to zero (see supplement for the proof).

Table 10: Maximum value of KL, L_1 and L_2 with corresponding value of ρ_w , for CDWC vs CDVM as base in (a), and CDWN vs CDVM as base in (b). The latter serves as a yard-stick reference.

(a) CDWC vs CDVM							(b) PDWN vs PDVM						
m	KL		L_1		L_2		m	KL		L_1		L_2	
	max	ρ_w	max	ρ_w	max	ρ_w		max	ρ_w	max	ρ_w	max	ρ_w
10	0.313	0.900	0.639	0.852	0.441	0.870	10	0.018	0.700	0.099	0.563	0.051	0.638
37	0.951	0.985	1.126	0.975	1.491	0.980	37	0.017	0.698	0.107	0.609	0.051	0.634
1000*	1.578	0.995	1.387	0.995	5.342	0.995	1000	0.017	0.698	0.107	0.604	0.051	0.634
10000*	1.571	0.995	1.388	0.995	5.187	0.995	10000	0.017	0.698	0.107	0.604	0.051	0.634

* emphasizes that the maximum value is higher.

Theorem 7.

Let f_v , f_c and f_n be the pdf of von Mises, wrapped Cauchy and wrapped normal with concentration parameters κ , ρ and σ^2 respectively. Let the parameters be mapped to each other based on their first trigonometric moments as

$$A(\kappa) = \rho = e^{-\sigma^2/2}, \text{ where } A(\kappa) = I_1(\kappa)/I_0(\kappa).$$

Then for large κ , we have

$$(i) \text{ } KL(f_v, f_c) \approx \frac{1}{2} \log(2\pi) - \frac{1}{2} + \int_{-\infty}^{\infty} \frac{e^{-z^2/2}}{\sqrt{2\pi}} \log\left(\frac{1}{4\sqrt{\kappa}} + \sqrt{\kappa}z^2\right) dz.$$

$$(ii) \text{ } KL(f_v, f_n) \approx 0.$$

7.3 Comparison among discrete models: marginalized and conditionalized

Ideally, the marginalized approach is applicable to grouped data, whereas the conditionalized approach is appropriate when the data is naturally discrete. Practically, the conditionalized approach is mathematically and computationally more easily tractable and may be used when we do not expect much difference from the analyses based on the two distributions. We note here that except for very small values of m such as $m < 10$, inference based on the conditionalized and marginalisation approaches will be similar. Figure 7 plots the probability functions of MDWC (dashed lines with crosses) and CDWC (solid line with circle) for $m = 10, 37$, different values of $\rho \in \{0.02, 0.25, 0.75\}$. For small values of m (e.g. 10) the two probability functions are different (mainly peakedness), but for larger m (e.g. 37) the two merge with each other across different ρ values.

In this paper, we have two practical examples, one for smart homes and another for roulette data from casinos. In the former case, marginalized approach is natural, whereas in the roulette the conditionalized approach is natural. However, as noted above, for moderately large m , the two approaches should lead to similar. Indeed, for the human activity data (see Section 6.2), we have verified that both the conditionalized and marginalized approaches lead to estimation of similar mixture components. However, for changepoint analysis with roulette data, since the domain is a regular lattice, we used the conditionalized approach.

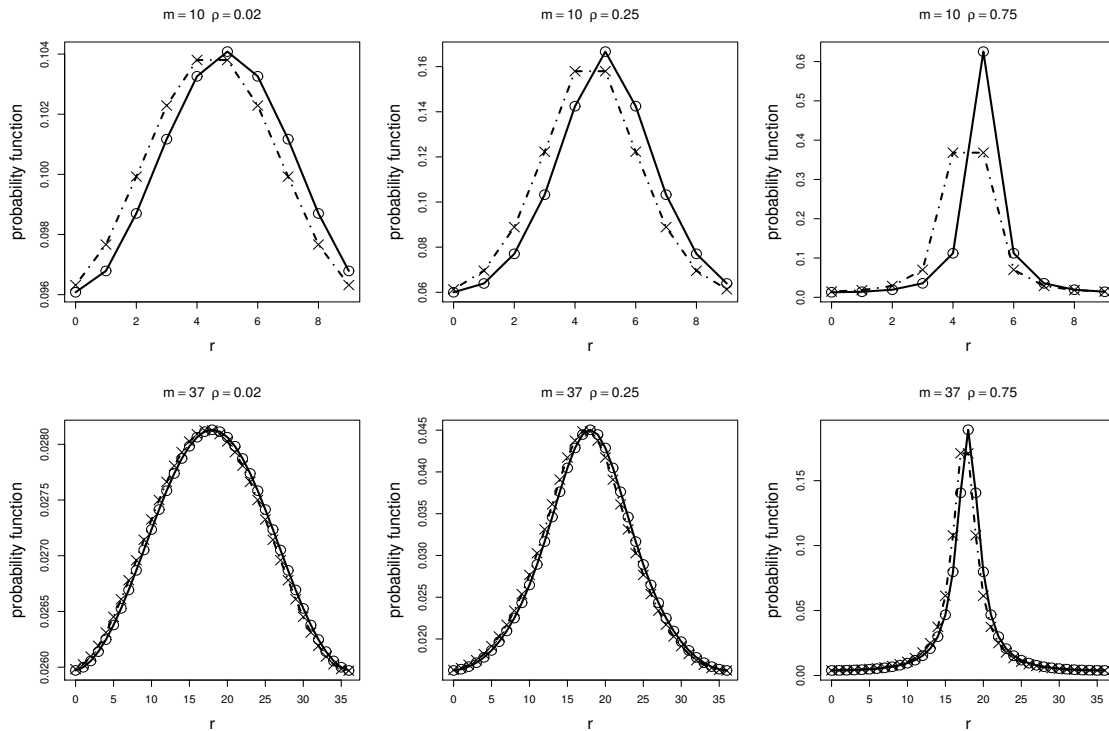


Figure 7: Comparison of probability functions of MDWC (dashed lines with crosses) and CDWC (solid line with circle) for $m = 10, 37$, different values of $\rho \in \{0.02, 0.25, 0.75\}$.

7.4 Sheppard correction: for discretization based on marginalized and conditioning

Circular discrete data could arise mainly from two sources. The first source is that the population is continuous but the observed values are often recorded/used in an aggregated form, e.g. grouped in bins or rounded appropriately. The second source, which is more natural where the population itself is discrete, such as for the roulette data. In the first case, there has been a recent survey by Humphreys and Ruxton (2017) to find out what are the most common values of m in aggregating. It turns out that the most common values of m are 4, 8, 12 and 36, which suggest that the assumption of a continuous distribution is often violated for data analysis.

Suppose we have circular data $\{\theta_i, i = 1, 2, \dots, n\}$ We first recap the Sheppard correction for the p th resultant length defined below, which is in general key element of any data analysis.

$$\bar{R}_p = \sqrt{\left(\frac{1}{n} \sum_{i=1}^n \cos(p\theta_i)\right)^2 + \left(\frac{1}{n} \sum_{i=1}^n \sin(p\theta_i)\right)^2}$$

For example, the Rayleigh test for uniformity is based on \bar{R}_1 . When the data is actually discrete, such as binned data, computing \bar{R}_p by treating it like continuous data may need the Sheppard correction. For example, Humphreys and Ruxton (2017), highlights several examples in ecology, where the data is binned and inference by treating it as continuous may not be appropriate. A general multiplier, when the data is discretized in bins of length h for

this correction is as follows (see Mardia 1972, pp.37 -38)

$$\tilde{\bar{R}}_p = a(ph)\bar{R}_p, \text{ where } a(h) = \frac{h}{2 \sin(h/2)}. \quad (95)$$

Here, we study the need for such a correction for the marginalized and conditionalized wrapped Cauchy distributions, if the data is treated as if it were from wrapped Cauchy. Table 11 shows trigonometric moments computed for $MDWC(m, \rho, t)$ and $CDWC(m, \rho, t)$ for $\rho = 0.5$, $t = 0$, for different values of m . As a reference, for wrapped Cauchy, $E \cos(\theta) = 0.5$ and $E \cos(2\theta) = 0.25$. Discretization matters for MDWC if m less than 20, i.e. bin with angle 18 degrees. Surprisingly effect is a bit smaller for CDWC. The overriding message is that Sheppard correction does not influence the conclusions based on the trigonometric moments unless the grouping is very coarse Mardia (1972). Our table gives a specific flavor of the effect rather than very broad Sheppard correction, which is generic. However, when the data is intrinsically discrete such as in the roulette case it will be essential to use a discrete distribution for correct inference such as in mixtures, changepoint.

Table 11: Trigonometric moments computed for $MDWC(m, \rho, t)$ and $CDWC(m, \rho, t)$ for $\rho = 0.5$, $t = 0$, for different values of m . As reference, for WC $E \cos(\theta) = 0.5$ and $E \cos(2\theta) = 0.25$.

m	MDWC*		CDWC	
	$E \cos(\theta)$	$E \cos(2\theta)$	$E \cos(\theta)$	$E \cos(2\theta)$
3	0.159	0.159	0.667	0.667
5	0.368	0.038	0.545	0.364
10	0.466	0.190	0.501	0.254
15	0.485	0.221	0.500	0.250
20	0.493	0.232	0.500	0.250
30	0.495	0.242	0.500	0.250
50	0.497	0.248	0.500	0.250
100	0.503	0.247	0.500	0.250
500	0.499	0.248	0.500	0.250

* For MDWC the moments were computed using simulated data of size 200000.

8 Extensions

First, we show how the marginalized and conditionalized discrete distributions (location family) extend to the irregular lattice support. Next we give a generalization of discrete circular distributions to a four parameter family. Further, we give some distributions on the torus based on a new bivariate wrapped Cauchy distribution, which has both marginal as well as conditional wrapped Cauchy (unlike for bivariate von Mises distributions); so we check whether such a property is inherited by the corresponding discrete distribution or not. Finally, we give a generalization of conditionalized discrete distributions to conditionalized discrete stable distributions.

8.1 A construction of location family supported on irregular lattice

We have considered so far marginalized or conditionalized discrete distributions on the regular lattice but the domain can be extended to irregular lattice as follows. We can rewrite the marginalized and conditionalized discrete probability function in equations (49) and (56) in terms of the angle $\theta \in \{2\pi r/m, r \in \mathbb{Z}_m\}$ as

$$\tilde{p}(\theta|m, \tau, t) = \int_{\theta}^{\theta+2\pi/m} g_{\tau}(\theta - 2\pi t/m) d\theta \quad \text{or} \quad \tilde{p}(\theta|m, \tau, t) = \frac{g_{\tau}(\theta - 2\pi t/m)}{\sum_{r=0}^{m-1} g_{\tau}(2\pi r/m)}. \quad (96)$$

We can then consider the following two component mixture

$$p \cdot \tilde{p}(\theta|m_1, \tau_1, t_1) + (1 - p) \cdot \tilde{p}(\theta|m_2, \tau_2, t_2), \quad \text{where } m_1 \neq m_2. \quad (97)$$

The mixture is supported on the union of the supports of the individual discrete distribution components, i.e.,

$$\theta \in \{2\pi r/m_1, r = 0, 1, 2, \dots, m_1 - 1\} \cup \{2\pi r/m_2, r = 0, 1, 2, \dots, m_2 - 1\}.$$

With this construction, we can create new rich classes of discrete circular distributions possibly supported on irregular lattices, with modes at different locations and with possibly dense distribution with several modes. Here, we provide a simple example to illustrate the concept. Consider a mixture of discrete distribution components with $m = 4$ and $m = 9$. The support for $m = 4$ is on angles $\{0, \pi/2, \pi, 3\pi/2\}$ and for $m = 9$ it is

$$\{0, 2\pi/9, 4\pi/9, 6\pi/9, 8\pi/9, 10\pi/9, 12\pi/9, 14\pi/9, 16\pi/9\}.$$

However, their mixture gives rise to a distribution with an irregular lattice support. Figure 8 plots the points on the circle that form the support for such a distribution. The points denoted by circles are in the support of the distribution with $m = 4$ and the points denoted by crosses are in the support of the distribution with $m = 9$. While each component is supported on a regular lattice, when these two components form a mixture, the support is an irregular lattice on the circle (see supplement for some interesting cases).

8.2 Four parameter families of discrete circular distributions

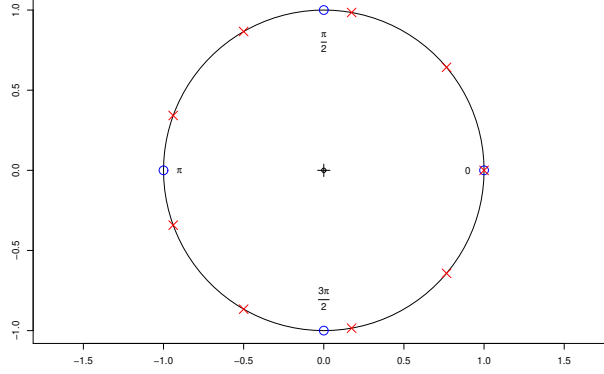
We follow the general family of circular distributions of Kato and Jones (2015), which includes wrapped Cauchy distribution. It has four parameters which controls its first four trigonometric moments leading to unimodal symmetrical as well as skew distributions as particular cases. This family also has an analytically tractable normalizing constant and its pdf is given by

$$g_{KJ}(\theta) = \frac{1}{2\pi} \left(1 + 2\gamma \frac{\cos(\theta - \mu) - \rho \cos \lambda}{1 + \rho^2 - 2\rho \cos(\theta - \mu - \lambda)} \right), \quad -\pi < \theta \leq \pi, \quad (98)$$

where the parameters are constrained by

$$0 \leq \rho < 1, 0 \leq \gamma \leq (1 + \rho)/2, -\pi \leq \mu, \lambda \leq \pi, \quad \text{and } \rho\gamma \cos \lambda \geq (\rho^2 + 2\gamma - 1)/2. \quad (99)$$

Figure 8: Irregular lattice support for mixture of discrete circular distribution components with $m = 4$ and $m = 9$. Support for $m = 4$ indicated by circles and for $m = 9$ by crosses.



The marginalized discrete distribution based on (98) (see for example Kato and Jones 2015, supplementary file) can be shown to have a closed form probability function given by

$$\begin{aligned}
& p(r|m, \rho, \mu, \gamma, \lambda) \\
&= \frac{1}{m} (1 - \gamma/\rho \cos \lambda) + \frac{\gamma \sin \lambda}{2\pi\rho} \log \frac{1 + \rho^2 - 2\rho \cos(2\pi r/m - \mu - \lambda)}{1 + \rho^2 - 2\rho \cos(2\pi(r+1)/m - \mu - \lambda)} \\
&+ \frac{\gamma \cos \lambda}{\pi\rho} \tan^{-1} \left(\frac{\frac{1+\rho}{1-\rho} (\tan(\pi(r+1)/m - \mu/2 - \lambda/2) - \tan(\pi r/m - \mu/2 - \lambda/2))}{1 + \left(\frac{1+\rho}{1-\rho}\right)^2 \tan(\pi(r+1)/m - \mu/2 - \lambda/2) \tan(\pi r/m - \mu/2 - \lambda/2)} \right) \\
&+ \frac{\gamma \cos \lambda}{\rho} (I_{\{\tan(\pi(r+1)/2 - \mu/2 - \lambda/2) < 1/\tan(\lambda/2)\}} - I_{\{\tan(\pi r/2 - \mu/2 - \lambda/2) < 1/\tan(\lambda/2)\}}), \\
& r \in \mathbb{Z}_m,
\end{aligned} \tag{100}$$

with the same constraints on parameters as in (99). We will call this family, the marginalized discrete Kato-Jones family, or briefly as MDKJ family. For $\lambda = 0$, a family of symmetric distributions is obtained with the probability function

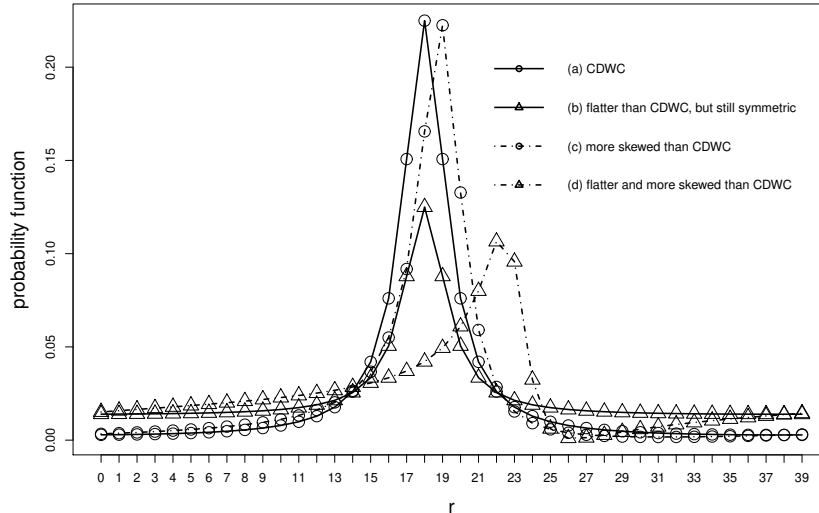
$$\begin{aligned}
& p(r|m, \rho, \mu, \gamma, \lambda = 0) \\
&= \frac{1 - \gamma/\rho}{m} + \frac{\gamma}{\pi\rho} \tan^{-1} \left(\frac{\frac{1+\rho}{1-\rho} \{\tan(\pi(r+1)/m - \mu/2) - \tan(\pi r/m - \mu/2)\}}{1 + \left(\frac{1+\rho}{1-\rho}\right)^2 \tan(\pi(r+1)/m - \mu/2) \tan(\pi r/m - \mu/2)} \right), \\
& r \in \mathbb{Z}_m.
\end{aligned} \tag{101}$$

The conditionalized discrete distribution from (98), is given by the probability function

$$p(r|m, \rho, \mu, \gamma, \lambda) = \frac{1}{D^*} \left(1 + 2\gamma \frac{\cos(\frac{2\pi r}{m} - \mu) - \rho \cos \lambda}{1 + \rho^2 - 2\rho \cos(\frac{2\pi r}{m} - \mu - \lambda)} \right), r \in \mathbb{Z}_m, \tag{102}$$

with the same constraints on parameters as in (99). We will call this family, the conditionalized discrete Kato-Jones family, or briefly as CDKJ family. The CDWC is obtained as a special

Figure 9: Probability function of CDKJ family for parameter values $m = 40, t = 18$, $\rho = 0.8$ and four different values of (γ, λ) : (a) $(0.8, 0)$ (solid line and circle), (b) $(0.4, 0)$ (solid line and triangle), (c) $(0.8, 2\pi/m)$ (dotted line and circle) and (d) $(0.4, 2\pi(m - 5)/m)$ (dotted line and triangle) respectively.



case when $\lambda = 0$ and $\gamma = \rho$. Note that the constraints ensure that the probability function in (98) is positive and hence also for the discretized version (102). The normalizing constant can be simplified as stated in the following theorem.

Theorem 8. *For the probability function (102), we have*

$$D^* = m \left(1 + 2\gamma\rho^{m-1} \frac{\cos(m(\mu + \lambda) - \lambda) - \rho^m \cos \lambda}{1 + \rho^{2m} - 2\rho^m \cos(m(\mu + \lambda))} \right). \quad (103)$$

The proof of this theorem is given in the supplement. We now give a plot in Figure 9 of typical particular cases of this CDKJ distribution. We have selected $m = 40, t = 18$ or $\mu = 2\pi \times t/m$, $\rho = 0.8$ and four different values of (γ, λ) : (a) $(0.8, 0)$, (b) $(0.4, 0)$, (c) $(0.8, 2\pi/m)$, (d) $(0.4, 2\pi(m - 5)/m)$. Note that (a) is “CDWC”. It can be seen now that the distribution (b) is “flatter than CDWC but still symmetric”, (c) is “more skewed than CDWC” and (d) is “flatter and more skewed than CDWC” respectively. Thus, the CDKJ family is also quite flexible like that of Kato and Jones (2015), including various type of symmetrical as well as skewed distributions.

It is to be noted that the Beran family (Beran 1979) provides generalization of von Mises distribution with exponent trigonometric functions of higher order and we can write conditionalized discrete Beran distributions. However, even in the simple case of four terms only (up to second order trigonometric function), it does not lead to a neat interpretation of parameters (see for example Gatto and Jammalamadaka 2007) though it allows for skewness.

8.3 Discrete distributions on the torus

Kato and Pewsey (2015) have given a bivariate Cauchy distribution on the torus with pdf of

the form

$$g(\theta_1, \theta_2) \propto (c_0 - c_1 \cos(\theta_1 - \mu_1) - c_2 \cos(\theta_2 - \mu_2) - c_3 \cos(\theta_1 - \mu_1) \cos(\theta_2 - \mu_2) - c_4 \sin(\theta_1 - \mu_1) \sin(\theta_2 - \mu_2))^{-1}, \quad (104)$$

$-\pi \leq \mu_1, \mu_2 \leq \pi$, $-\pi \leq \mu_1, \mu_2 \leq \pi$. This is one of the only known distribution which has both marginals and conditionals of the same form, namely wrapped Cauchy. Indeed, a multivariate version of (104), which we call ‘‘multivariate wrapped Cauchy’’ (MWC) will be of the form

$$g(\theta_1, \theta_2, \dots, \theta_d) \propto \left(c_0 + \kappa^T \cos(\boldsymbol{\theta} - \boldsymbol{\mu}) + [\cos \boldsymbol{\theta} \quad \sin \boldsymbol{\theta}] \Sigma^{-1} \begin{bmatrix} \cos \boldsymbol{\theta} \\ \sin \boldsymbol{\theta} \end{bmatrix} \right)^{-1}, \quad (105)$$

where $\boldsymbol{\theta} = (\theta_1, \theta_2, \dots, \theta_d)^T$, $\boldsymbol{\mu} = (\mu_1, \mu_2, \dots, \mu_d)^T$ and $\Sigma^{-1} = \begin{bmatrix} \Sigma_{11} & \Sigma_{12} \\ \Sigma_{21} & \Sigma_{22} \end{bmatrix}$ is a positive definite matrix.

A particular case of interest is

$$g(\theta_1, \theta_2, \dots, \theta_d) \propto \frac{1}{c_0 + \sum_{i=1}^d \sum_{j=1}^d c_{ij} \cos(\theta_i - \theta_j - \mu_{ij})}. \quad (106)$$

Furthermore, the generalized multivariate von Mises distribution (gMVM) is given by the pdf

$$g(\theta_1, \theta_2, \dots, \theta_d) \propto \exp \left\{ c_0 + \kappa^T \cos(\boldsymbol{\theta} - \boldsymbol{\mu}) + [\cos \boldsymbol{\theta} \quad \sin \boldsymbol{\theta}] \Sigma^{-1} \begin{bmatrix} \cos \boldsymbol{\theta} \\ \sin \boldsymbol{\theta} \end{bmatrix} \right\}. \quad (107)$$

This is a particular case of the distribution given by Khatri and Mardia (1977) which is the generalized multivariate von Mises distribution, see also (Navarro et al., 2017). For $\Sigma_{12} = \Sigma_{21} = \mathbf{0}$, we get the distribution of Mardia and Patrangenaru (2005). Thus from equations (105) and (107), we can obtain the corresponding marginalized and conditionalized discrete distributions with the random variable θ_i replaced by $2\pi r_i/m$ for $i = 1, 2, \dots, d$.

Obtaining the marginalized discrete generalized von Mises (MDgMVM) distribution from (107) would involve evaluation of multiple integration, which would need to be done numerically. However, one of the key advantages of this construction is that normalizing constant is automatically taken care and further the marginal distributions will be univariate MDgVM.

The conditionalized discrete generalized von Mises (CDgMVM) is given by

$$p(2\pi \mathbf{r}/m) \propto \exp \left\{ c_0 + \kappa^T \cos(2\pi \mathbf{r}/m - \boldsymbol{\mu}) + [\cos(2\pi \mathbf{r}/m) \quad \sin(2\pi \mathbf{r}/m)] \Sigma^{-1} \begin{bmatrix} \cos(2\pi \mathbf{r}/m) \\ \sin(2\pi \mathbf{r}/m) \end{bmatrix} \right\}. \quad (108)$$

The conditional distributions, i.e. $r_i | (r_1, \dots, r_{i-1}, r_{i+1}, \dots, r_k)$ for each i will be CDVM. Also, being in the exponential family, we can write a conjugate prior following standard approach (see for example Mardia 2010)

We now discuss below, the bivariate case and some properties. It is expected following Kato and Pewsey (2015) and Kent and Tyler (1988), that it should be useful when we seek robust estimates. Kato and Pewsey (2015) have stated that ‘‘the bivariate Cauchy distribution should be useful when the frequency of data some distance from the mode is relatively high’’ (in contrast to the bivariate von Mises distribution of Mardia (1975a)).

8.3.1 Bivariate case

We start with the simplest bivariate case given in equation (5) of Kato and Pewsey (2015) (which is the distribution first introduced by Kato (2009)), i.e.

$$g(\theta_1, \theta_2) = \frac{1}{4\pi^2} \frac{1}{1 + \rho^2 - 2|\rho| \cos(q\theta_1 - \theta_2 - \mu)}, \quad -\pi < \theta_1, \theta_2 \leq \pi, \quad (109)$$

where $q = \text{sgn}(\rho)$ ($q = \pm 1$), $-\pi < \mu \leq \pi$ and $-1 < \rho < 1$. For simplicity take $\rho > 0$; so $q = 1$. Note that here the marginal distributions are uniform and the conditional distributions are wrapped Cauchy.

Using equation (38), the bivariate marginalized discrete distribution can be written as

$$\begin{aligned} p(r_1, r_2 | m, \rho, \mu) &= \frac{1}{2\pi} \int_{2\pi r_1/m}^{2\pi(r_1+1)/m} \frac{1}{2\pi} \int_{2\pi r_2/m}^{2\pi(r_2+1)/m} \frac{d\theta_1}{1 + \rho^2 - 2\rho \cos(\theta_1 - \theta_2 - \mu)} d\theta_2 \\ &= \frac{1}{2\pi} \int_{2\pi r_1/m}^{2\pi(r_1+1)/m} \frac{1}{\pi} \tan^{-1} \left(\frac{1+\rho}{1-\rho} \tan(\pi(r_2+1)/m - \mu/2 - \theta_2/2) \right) d\theta_2 \\ &\quad - \frac{1}{2\pi} \int_{2\pi r_1/m}^{2\pi(r_1+1)/m} \frac{1}{\pi} \tan^{-1} \left(\frac{1+\rho}{1-\rho} \tan(\pi r_2/m - \mu/2 - \theta_2/2) \right) d\theta_2 \end{aligned}$$

This can be further simplified as

$$p(r_1, r_2 | m, \rho, \mu) = v(u(r_1 - r_2), u(r_1 - r_2 + 1)) - v(u(r_1 - r_2 - 1), u(r_1 - r_2)), \quad (110)$$

where

$$v(k_1, k_2) = \frac{1}{2\pi^2} \frac{1-\rho}{1+\rho} \int_{u(k_1)}^{u(k_2)} \frac{\tan^{-1} u}{1 + \left(\frac{1-\rho}{1+\rho}\right)^2 u^2} du, \quad \text{with } u(k) = \frac{1+\rho}{1-\rho} \tan(\pi k/m + \mu/2).$$

The probability function (110) does not admit a closed form and would need to be computed numerically. Note that

$$\sum_{r_2=0}^{m-1} p(r_1, r_2 | m, \rho, \mu) = \int_{-\pi}^{\pi} g(2\pi r_1/m, \theta_2) d\theta_2 = \frac{1}{2\pi} \int_{2\pi r_1/m}^{2\pi(r_1+1)/m} d\theta_1 = \frac{1}{m}.$$

So, the marginal distributions will be uniform on the lattice. The conditional distribution of $r_1 | r_2$ is therefore given by

$$p(r_1 | r_2, m, \rho, \mu) = \frac{p(r_1, r_2 | m, \rho, \mu)}{\sum_{r_1=0}^{m-1} p(r_1, r_2 | m, \rho, \mu)} = m p(r_1, r_2, m, \rho, \mu), \quad r_1 \in \mathbb{Z}_m,$$

which is proportional to the right hand side of (110). So, the conditional distribution is not MDWC.

The bivariate conditionalized discrete distribution from equation (109) is more easily tractable and can be written as

$$p(r_1, r_2 | m, \rho, \mu) = \frac{1}{D^{**}} \frac{1}{1 + \rho^2 - 2\rho \cos(2\pi(r_1 - r_2)/m - \mu)}, \quad (111)$$

where the normalizing constant is derived in the supplement as

$$D^{**} = \frac{m^2(1 - \rho^{2m})}{(1 - \rho^2)(1 + \rho^{2m} - 2\rho^m \cos(m\mu))}. \quad (112)$$

Using the same formula it can be shown that the marginal distributions are uniform on the lattice. Also, it is easy to see that the conditional distributions are CDWC. This is also true with $q = -1$.

The key point is that equation (109) is the building block of Kato-Pewsey distribution which has been obtained by using general Möbius transformation (see also Downs and Mardia (2002)). The mapping is (θ_1, θ_2) to the new variables (ϕ_1, ϕ_2) defined by

$$\theta_i = \nu_i + 2 \arctan \left(\frac{1 + \xi_i}{1 - \xi_i} \right) \tan \left(\frac{\phi_i - \mu - \nu_i}{2} \right), \quad i = 1, 2. \quad (113)$$

However, the Möbius transformation is a nonlinear transformation; so (ϕ_1, ϕ_2) from θ_1, θ_2 do not get mapped to the lattice and in particular the resulting points are not equispaced so the mapped bivariate CDWC is not expected to have the marginals CDWC. Indeed, we have the following result starting from the conditionalized discrete version from equation (104).

Theorem 9. *The general 6-parameter distribution with conditionalized discrete version of Kato-Pewsey bivariate distribution on the torus has conditional distributions as CDWC but cannot have marginals as CDWC, except for some trivial cases.*

A similar result applies for the multivariate (CDgMWC) case, i.e., the conditionals are CDWC, but not the marginals.

8.4 Conditionalized discrete wrapped stable distributions

The wrapped Cauchy distribution generalises to wrapped stable distributions (see, for example, Mardia and Jupp (2000)), which has the probability density function

$$f_s(\theta) = \frac{1}{2\pi} \left\{ 1 + 2 \sum_{q=1}^{\infty} [\rho^{q^a} \cos\{q(\theta - \mu) + bq^a\}] \right\}, \quad \theta, \mu \in [0, 2\pi), \quad \rho \in [0, 1), \quad 0 < a \leq 2 \quad (114)$$

The wrapped stable distributions with $b = 0$ include the wrapped normal ($a = 2$) and the wrapped Cauchy ($a = 1$) distributions. In the case $b = 0$, the distribution has a unique mode at μ , as it is a particular case of the circular location family. The corresponding conditionalized discrete wrapped stable distribution of equation (114), is obtained on replacing θ by $\theta = 2\pi r/m$ and μ by $2\pi t/m$, and the probability function is given by

$$p(r) = \frac{1 + 2 \sum_{q=1}^{\infty} [\rho^{q^a} \cos\{q(2\pi(r - t)/m) + bq^a\}]}{\sum_{r=0}^{m-1} \left\{ 1 + 2 \sum_{q=1}^{\infty} [\rho^{q^a} \cos\{q(2\pi(r - t)/m) + bq^a\}] \right\}}, \quad r, t \in \mathbb{Z}_m. \quad (115)$$

For $b = 0$, it can be shown that we get the symmetrical distribution with the probability function

$$p(r|m, \rho, t, a) = \frac{1 + 2 \sum_{q=1}^{\infty} [\rho^{q^a} \cos\{q(2\pi(r - t)/m)\}]}{m(1 + 2 \sum_{k=1}^{\infty} \rho^{(mk)^a}}, \quad r, t \in \mathbb{Z}_m, \quad \rho \in [0, 1), \quad a \in (0, 2]. \quad (116)$$

Its characteristic function is given by the following theorem (see supplement for the proof).

Theorem 10. *The characteristic function of the probability function (116) is given by*

$$E \left[e^{ip \frac{2\pi x}{m}} \right] = e^{ip \frac{2\pi t}{m}} \psi_{p,m}, \quad (117)$$

where

$$\psi_{p,m} = \frac{\rho^{p^a} + \sum_{k=1}^{\infty} (\rho^{(km-p)^a} + \rho^{(km+p)^a})}{1 + 2 \sum_{k=1}^{\infty} \rho^{(km)^a}}, \quad \text{for } p(\text{mod } m). \quad (118)$$

9 Discussion

In this paper, we have given various ways of constructing families of discrete circular distributions and have selected the marginalized and conditionalized approaches for our analysis, but the other constructions described above can be explored further. Sometimes we have selected marginalized or conditionalized, and von Mises or wrapped Cauchy discrete distributions. We note that such a situation of using two distributions for different practical applications is not uncommon in directional statistics. Indeed, Kendall (1974) made a similar case when using von Mises vs wrapped normal distribution (the lumped Gaussian distribution):

“For analytical, computational, and statistical purposes it is sometimes the lumped Gaussian distribution which is the more convenient, and sometimes the von Mises. As they are practically indistinguishable, we shall have (and will accept) the option of using sometimes one, and sometimes the other, and we shall change horses more than once in crossing the broad stream that lies before us.”

However, the situation is a bit more involved here since we have competitive discrete distributions from the two families. In Section 7, we have carried out various comparisons to deal with these and related inferential questions.

The marginalized and conditionalized families of distributions have a significant potential for further development. In fact we have already pointed out a characterization on line that the two approaches lead to the same distribution if and only if the parent is the exponential distribution. We have some analogous results for the discrete circular case.

In Section 8 we have introduced the conditionalized circular stable distributions, marginalized and conditionalized Kato-Jones distribution and bivariate discrete distributions on the torus, but further work can be done in various directions, such as dealing with inference problems and data analysis. We have extended the model to higher manifolds on torus with discrete support but we have left as an open problem on how to extend the model to hypersphere for example; this temptation has been resisted as we have not had any motivating practical applications.

Supplementary material

Supplementary materials may be requested from the authors. More details and explanation will be available in the forthcoming monograph Mardia and Sriram (2020).

Acknowledgments

We wish to thank Arthur Pewsey for some help with R, Eris Chinellato for help with the humane activity data and CHAD, to John Kent, Peter Green and John Wootton for some

discussions. The first author would also like to thank the Leverhulme Trust for the Emeritus Fellowship.

References

Beran, R. (1979) Exponential models for directional data. *Annals of Statistics*, **7**, 1162–1178.

CHAD (2002) Extracting human activity information from chad on the pc. u.s. environmental protection agency, washington. <https://www.epa.gov/healthresearch/consolidated-human-activity-database-chad-use-huma>

Chinellato, E., Mardia, K. V., Hogg, D. and Cohn, A. (2017) An incremental von mises mixture framework for modelling human activity streaming data. *Proceedings International work-conference on Time Series (ITISE 2017.)*, 379–389.

Downs, T. D. and Mardia, K. V. (2002) Circular regression. *Biometrika*, **89**, 683–698.

Fisher, N. I. (1993) *Statistical Analysis of Circular Data*. Cambridge University Press.

Fisher, N. I., Lewis, T. and Embleton, B. (1987) *Statistical Analysis of Spherical Data*. Cambridge University Press.

Gatto, R. and Jammalamadaka, S. R. (2007) The generalized von mises distribution. *Statistical Methodology*, **4**, 341–353.

HOWZ (n.d.) Link to howz: A smart home for the elderly <https://www.edf.fr/en/howz-smart-home-senior-citizens>.

Humphreys, R. K. and Ruxton, G. D. (2017) Consequences of grouped data for testing for departure from circular uniformity. *Behavioral Ecology and Sociobiology*, **71**, 167.

Inusah, S. and Kozubowski, T. J. (2006) A discrete analogue of the laplace distribution. *Journal of Statistical Planning and Inference*, **136**, 1090–1102.

Jammalamadaka, R. and Sengupta, A. (2001) *Topics in Circular Statistics*. Chapman and Hall/CRC.

Jayakumar, K. and Jacob, S. (2012) Wrapped skew laplace distribution on integers: a new probability model for circular data. *Open Journal of Statistics*, **2**, 106–114.

Joe, H. (2014) *Monographs on Applied Statistics and Probability*. CRC Press, Taylor Francis Group, Chapman and Hall.

Johnson, R. A. and Wehrly, T. E. (1978) Some angular-linear distributions and related regression models. *Journal of American Statistical Association*, **73**, 602–606.

Jolley, L. B. W. (1961) *Summation of Series*. Dover Publications Inc, New York.

Jones, M. C., Pewsey, A. and Kato, S. (2015) On a class of circulars: copulas for circular distributions. *Annals of the Institute of Statistical Mathematics*, **67**, 843–862.

- Kato, S. (2009) A distribution for a pair of unit vectors generated by brownian motion. *Bernoulli*, **15**, 898–921.
- Kato, S. and Jones, M. C. (2015) A tractable and interpretable four-parameter family of unimodal distributions on the circle. *Biometrika*, **102**, 181–190.
- Kato, S. and Pewsey, A. (2015) A möbius transformation-induced distribution on the torus. *Biometrika*, **102**, 359–370.
- Kemp, A. W. (1997) Characterizations of a discrete normal distribution. *Journal of Statistical Planning and Inference*, **63**, 223–229.
- Kendall, D. G. (1974) Hunting quanta. *Philosophical Transactions of the Royal Society of London. Series A, Mathematical and Physical Sciences*, **276**, 231–266.
- Kent, J. T. and Tyler, D. E. (1988) Maximum likelihood estimation for the wrapped cauchy distribution. *Journal of Applied Statistics*, **15**, 247–254.
- Khatri, C. G. and Mardia, K. V. (1977) The von mises-fisher matrix distribution in orientation statistics. *Journal of Royal Statistical Society B*, **34**, 95–106.
- Ley, C. and Verdebout, T. (2017) *Modern Directional Statistics*. Chapman and Hall/CRC.
- (2018) *Applied Directional Statistics, Modern Methods and Case Studies*. Chapman and Hall/CRC.
- Mardia, K. V. (1972) *Statistics of Directional Data*. Academic Press, London.
- (1975a) Statistics of directional data (with discussion). *Journal of Royal Statistical Society B*, **37**, 349–393.
- (1975b) Characterizations of directional distributions. In G. P. Patil, S. Kotz and J. K. Ord (eds), *Statistical Distributions in Scientific Work*, **3**, 365–385 Reidel, Dordrecht. (55, 171, 262).
- (2010) Bayesian analysis for bivariate von mises distributions. *Journal of Applied Statistics*, **37**, 515–528.
- Mardia, K. V. and Jupp, P. E. (2000) *Directional Statistics*. Wiley.
- Mardia, K. V. and Patrangenaru, V. (2005) Directions and projective shapes. *The Annals of Statistics*, **33**, 1666–1699.
- Mardia, K. V. and Sriram, K. (2020) “Circular Statistics for Discrete Data with R” *Research Monograph (in preparation)*.
- Mastrantonio, G., Jona Lasinio, G., Maruotti, A. and Calise, G. (2019) Invariance properties and statistical inference for circular data. *Statistica Sinica*, **29**, 67–80.
- Navarro, A. K. W., Frelsen, J. and Turner, R. E. (2017) The multivariate generalised von mises distribution: inference and applications. *ArXiv working paper: <https://arxiv.org/abs/1602.05003>*.

- Papadatos, N. (2018) The characteristic function of the discrete cauchy distribution. *ArXiv link* <https://arxiv.org/abs/1809.09443>.
- Pewsey, A. and García-Portugués, E. (2020) Recent advances in directional statistics. *ArXiv* <https://arxiv.org/abs/2005.06889>.
- Pewsey, A. and Jones, M. C. (2005) Discrimination between the von mises and wrapped normal distributions: just how big does the sample size have to be? *Statistics*, **39**, 81–89.
- Pewsey, A., Neuäuser, M. and Ruxton, G. D. (2013) *Circular Statistics in R*. Oxford University Press.
- Szabłowski, P. J. (2001) Discrete normal distribution and its relationship with jacobi theta functions. *Statistics and Probability Letters*, **52**, 289–299.
- Watson, G. S. and Beran, R. J. (1967) Testing a sequence of unit vectors for serial correlation. *Journal of Geophysical Research*, **72**, 5655–5659.